University of Illinois at Urbana-Champaign

ACRC

Air Conditioning and Refrigeration Center A National Science Foundation/University Cooperative Research Center

A Simple Approach to Performance Analysis of Alternative Refrigerant Rolling-Piston-Type Rotary Compressors

M.-H. Kim and C. W. Bullard

ACRC CR-34 March 2001

For additional information:

Air Conditioning and Refrigeration Center
University of Illinois
Mechanical & Industrial Engineering Dept.
1206 West Green Street
Urbana, IL 61801

(217) 333-3115

The Air Conditioning and Refrigeration Center was founded in 1988 with a grant from the estate of Richard W. Kritzer, the founder of Peerless of America Inc. A State of Illinois Technology Challenge Grant helped build the laboratory facilities. The ACRC receives continuing support from the Richard W. Kritzer Endowment and the National Science Foundation. The following organizations have also become sponsors of the Center.

Amana Refrigeration, Inc.
Arçelik A. S.
Brazeway, Inc.
Carrier Corporation
Copeland Corporation
Dacor
Daikin Industries, Ltd.
DaimlerChrysler Corporation
Delphi Harrison Thermal Systems
Frigidaire Company
General Electric Company
General Motors Corporation
Hill PHOENIX
Honeywell, Inc.
Hussmann Corporation
Hydro Aluminum Adrian, Inc.
Indiana Tube Corporation
Invensys Climate Controls
Kelon Electrical Holdings Co., Ltd.
Lennox International, Inc.
LG Electronics, Inc.
Modine Manufacturing Co.
Parker Hannifin Corporation
Peerless of America, Inc.
Samsung Electronics Co., Ltd.
Tecumseh Products Company
The Trane Company
Thermo King Corporation
Valeo, Inc.
Visteon Automotive Systems
Wolverine Tube, Inc.
York International, Inc.

For additional information:

Air Conditioning & Refrigeration Center
Mechanical & Industrial Engineering Dept.
University of Illinois
1206 West Green Street
Urbana, IL 61801

217 333 3115

Abstract

A simple semi-empirical model for small rolling-piston-type rotary compressors using the most potential alternative refrigerants R-410A and R-407C including R-22 has been developed based on thermodynamic principles and large data sets from the compressor calorimeter test. The basic purpose of the compressor sub-model in a larger system model is to provide the refrigerant mass flow rate, power consumption and discharge states of the compressor using some given information. The input data are compressor geometry (displacement and clearance volume), compressor speed, suction pressure and temperature, discharge pressure, and ambient temperature as well as mass flow rate, power consumption, shell and discharge temperatures which are needed only for estimating the constants in the model. A mass flow rate model reflects clearance volumetric efficiency and simulates suction gas heating using an effectiveness method. Compressor work is calculated using the compressor efficiency represented by two empirical parameters. Compressor heat loss and a linear relationship between the discharge and shell temperatures are used for calculating the discharge temperature. The model proposed here is a general but simple and can predict the mass flow rate and power consumption and discharge temperature within the RMS errors of ±3% and ±2.8°C, respectively.

Table of Contents

List of Figures

List of Tables

Nomenclature

A B,C,D	= diameters in Fig. 2 (m)
C	= clearance volume ratio
H	= cylinder height (m)
h	= specific enthalpy (W/kg)
$\dot{m}$	= refrigerant mass flow rate (kg/h)
N	= number of data points
P	= pressure (kPa)
Q	= heat transfer rate from shell (W)
s	= specific entropy (kJ/kg oC)
T	= temperature (oC)
UA	= overall heat transfer coefficient (W/m2 oC)
Vdisp	= cylinder displacement (m3)
Vdot	= compressor volume flow (m3/sec)
v	= specific volume (m3/kg)
W	= compressor work (W)

Greek Symbols

α	= compensation factor in Eq. (3)
ε	= effectiveness
η_c	= isentropic compressor efficiency
η_v	= clearance volumetric efficiency
ω	= compressor speed (rpm)

Subscripts

amb	= ambient
cal	= calculation
cond	= condenser
dis	= compressor shell discharge
dp	= cylinder discharge port
evap	= evaporator
exp	= experimental
shaft	= compressor shaft
shell	= compressor shell
sp	= cylinder suction port
suc	= compressor shell suction

1. Introduction

The compressor is one of major components of an air conditioning system and has an important role on system energy efficiency. The high-side-sump rolling-piston-type rotary compressors are widely used as the compressors for the small-size residential air conditioning units because of their higher performance such as lower noise and discharge gas fluctuations compared to reciprocating type, especially in Asian and European countries.

Compressor manufacturers usually provide empirical performance curves called compressor maps, expressing refrigerant mass flow (or cooling capacity) and compressor power input as polynomial functions of evaporation temperature for a range of condensing temperatures. Since the compressor maps are based on fixed ambient and suction gas temperatures, they are useful for comparing and selecting the compressors. However, they are inadequate for general system analysis, because they contain no information about the effects of different ambient and suction temperatures and are unable to predict discharge temperatures, which define the condenser inlet condition. There are several detailed compressor models in the open literature, but they usually require large sets of unknown parameters to characterize the complicated refrigerant flow, heat exchanges, effects of oil, moving boundaries, and data on the geometry and heat transfer characteristics of internal parts. Most such models contain too little data to distinguish accurate parameter estimation from merely "tuning" the model for a few selected operating conditions. In addition, the use of HCFC refrigerant, R22, has been regulated and the performance data of alternative refrigerant compressors are important to system designer. The research project has been focusing on this issue in order to establish a foundation for the development of a simple physical model of alternative refrigerant rotary compressors, suitable for use in a/c simulation models.

The basic simple physical model [1] was developed based on thermodynamic principles and large data sets from compressor calorimeter and *in-situ* tests [2, 3]. There have been some attempts to add some corrections to the empirical performance curves provided by compressor manufacturers. Dabiri and Rice [4] suggested additional assumptions to account for suction gas heating, which have been used with limited success for reciprocating compressors with low-side sumps, and with greater success for rotary compressors where the suction gas is injected directly [5]. Haider et al. [6] investigated the effect of compressor map and ambient temperature on the power consumption of a refrigerator-freezer using the ERA (EPA Refrigerator Analysis) software, complemented by measured compressor and refrigerator-freezer data. They reported the accuracy of ERA estimation could be improved up to 5.1% at an ambient temperature of 43.3^{o}C by using the measured map data at 43.3^{o}C rather than the given map at standard test condition of 32.2^{o}C.

There are several detailed physical models of compressors in the literature. Prakash and Singh [7] developed a mathematical model for a reciprocating compressor using the first law of thermodynamics and assuming the refrigerant is an ideal gas. Hiller and Glicksmann [8] reported a detailed compressor model of reciprocating compressors and compared the simulation results with experimental data. Domanski and Didion [9] developed a quite detailed compressor model for a system simulation, but it requires over 30 input parameters. Todescat et al. [10] presented a thermal energy analysis of a reciprocating hermetic compressor using the energy balances for several parts of the compressor. They reported the effect of compressor shell temperature on the compressor performance such as power consumption and energy efficiency ratio. Recently, Cavallini et al. [11]

presented a steady state model for the thermal analysis of an hermetic reciprocating compressor and compared with a few experimental data points for R-134a and R-600a compressors. Rigola et al. [12] presented an advanced numerical scheme of the thermal and fluid dynamic behavior of small hermetic reciprocating compressors, along with some empirical data. Those models usually require large sets of unknown parameters to characterize the complicated refrigerant flow, heat exchanges, effects of oil, and moving boundaries, plus data on the geometry and heat transfer characteristics of internal parts. Most such papers contain too little data to distinguish accurate parameter estimation from merely "tuning" the model for a few selected operating conditions. Jahnig et al. [13] developed a model similar to that presented here, which embodies different physical assumptions underlying the mass flow and power submodels.

The purpose of this study is to extend to a different type of rolling-piston-type compressors using the most potential alternative refrigerants R410A and R407C including R22, on approach explored first for small hermetic reciprocating compressors [1], and to provide a simple but accurate semi-empirical compressor model to the system designer. Pressure losses along the refrigerant path are neglected and the compression process is assumed as isentropic. A mass flow rate model reflects clearance volumetric efficiency and simulates suction gas heating using an effectiveness method. Compressor work is calculated using an isentropic compressor efficiency represented by only two empirical parameters. A linear relationship between the discharge and shell temperatures is extracted from the data and used for calculating the discharge temperature for any ambient air temperature.

2. Rotary compressor

The simple description for the rotary compressors will be given here based on the references [14-16]. The rotary compressors are positive displacement machines and two designs of high-side sump rotary compressors are in common use, a rolling-piston-type (Figs. 1 and 2) and a rotating-vane–type (Fig. 3). The rolling-piston-type rotary compressor has a roller mounted on the eccentric of a shaft with a single vane in the cylinder block. The suction and discharge ports are located in the cylinder wall near the vane slot, but on opposite sides. The suction and discharge vapors are separated in the cylinder at the contact point between the roller and the cylinder and the vane held against the roller by a spring. The contact point between the cylinder wall and the roller changes continuously as the roller travels around the cylinder. The refrigerant vapor at low pressure and temperature enters directly the suction port of the cylinder through piping, and the compressed gas is directed into the compressor shell. Thus in case of the high-side sump compressors the entire compressor is at high discharge pressure. The refrigerant vapor flows continuously through both the suction and discharge ports, except for the instant the roller covers one or the other of the ports.

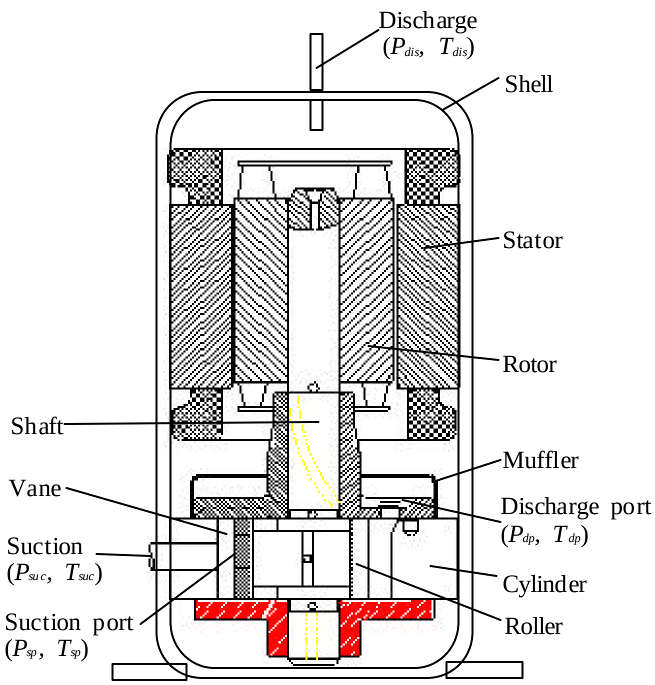

Figure 1. Schematic diagram of a rolling-piston-type rotary compressor

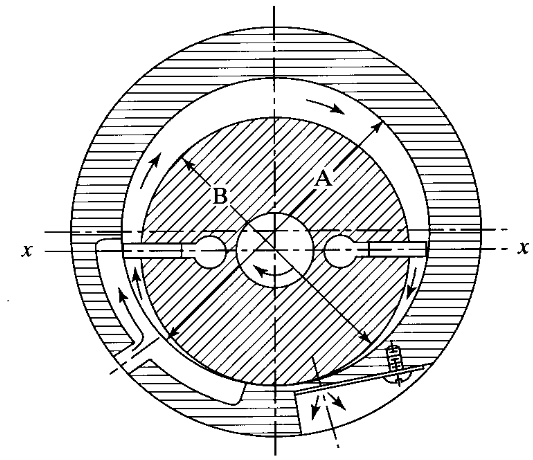

Figure 2. Rolling-piston-type rotary compressor

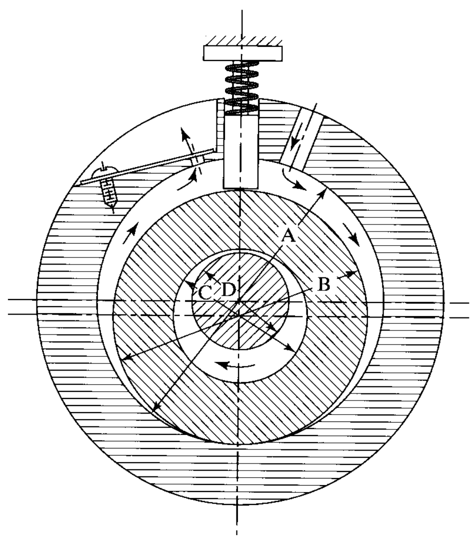

Figure 3. Rotating-vane-type rotary compressor

The compressor displacement is given by the difference in volume between the roller of diameter *B* and cylinder of diameter *A* as shown in Fig. 2.

$$V_{disp} = \frac{pH}{4}(A^2 - B^2) \quad (1)$$

where *H* is the cylinder height. This compressor has a flexing reed-type discharge valve, but no suction valve is needed. The discharge valve prevents refrigeration migration (the high pressure discharge gas from leaking back to the evaporator) through the compressor and suction line when the compressor cycles off.

The compressor volumetric flow rate can be obtained from the displacement and shaft speed if the roller inner diameter is equal to the shaft diameter, neglecting the slip between the surfaces

$$V_{dot} = \frac{v_{shaft} V_{disp}}{60} \quad (2)$$

Because the scope of the study is limited to the rolling-piston-type rotary compressors, we will only briefly describe the rotating-vane-type compressor. The rotating-vane-type rotary compressor has a series of vanes (usually two or more), which are installed equidistant around the periphery of a slotted rotor. The rotor shaft is mounted eccentrically in the cylinder so that the rotor contacts the cylinder wall on one side and the vanes move back and forth in the slots as the rotor shaft rolls around the cylinder wall. The refrigerant vapor enters into the cylinder through the suction port and is compressed by the reduction of the volume of the pockets as the rotor turns. The compressed vapor discharges into the compressor shell through the discharge port in the cylinder.

As the rolling-piston-type compressor, the rotating-vane-type compressor has no suction valve and has a discharge valve, which protects refrigeration migration through the compressor and suction line during the compressor off-cycle.

3. Simple compressor model

The basic purpose of the compressor sub-model in a larger system model is to provide the refrigerant mass flow rate, power consumption and discharge states of the compressor using some given information. The usual input data are compressor geometry (displacement and clearance volume), compressor speed, suction pressure and temperature, discharge pressure, and ambient temperature.

A detailed thermodynamic model of a compressor is extremely complex due to the inherently complicated structure of the compressor and refrigerant flow pathways, along which heat transfer and pressure vary substantially and rapidly. For some applications (e.g. design of variable-speed drives) such detailed modeling is necessary [17]. Our hypothesis is that the requirements for quasi-steady system simulation modeling are much less demanding, so several assumptions can be made to simplify the physical model for small hermetic rolling-piston-type rotary compressors:

(1) The refrigerant path can be treated as a steady state flow;
(2) The compression process is isentropic;
(3) The kinetic and potential energies of refrigerant are neglected;
(4) The pressure losses along the refrigerant path are neglected;
(5) The oil effects on the refrigerant properties are neglected.

The physical model is almost same as that used for the reciprocating compressor [1], so brief description will be given here.

For a given compressor velocity and volume flow rate, the mass flow rate for the rotary compressor can be calculated using the volumetric efficiency.

$$\dot{m} = 60\frac{h_v V_{dot} a}{v_{sp}} \tag{3}$$

where a is a compensation factor associated with the compressor speed, leakage and the uncertainty of compressor geometry (displacement and clearance volume) and it is to be estimated from Eq. (6).

Neglecting the leakage, the (clearance) volumetric efficiency for the compressors is given by Eq. (4), which accounts for re-expansion of the gas remaining in the clearance volume.

$$h_v = 1 - C\left(\frac{v_{sp}}{v(P_{dp}, s_{sp})} - 1\right) \tag{4}$$

When the displacement and clearance volume are known, the compensation factor, a is estimated, and provides insight into variation of motor speed and then unknown factors. However if these parameters are unknown, Eq. (6) yields an estimate of the product (V_{dot} a), with no loss of overall accuracy of the model. For a small hermetic compressor, we assume compression and re-expansion processes to be isentropic so the specific volume at the discharge port of the cylinder can be calculated. The increase in specific volume due to suction gas heating and mixing between the suction to the suction port has some effect on the volumetric efficiency and mass flow rate, even though the refrigerant vapor enters directly into the cylinder through suction port. We assume that both the direct effect (suction gas contact with hot metal) and indirect effect (mixing with heated plenum gas) are driven by the same maximum temperature differential within the subsystem boundary between suction and discharge lines:

$$e = \frac{h_{sp} - h_{suc}}{h(P_{sp}, T_{dp}) - h_{suc}} \tag{5}$$

The maximum enthalpy at the suction port of the cylinder is determined using the suction port's pressure and the maximum discharge temperature, which is based on the assumption of isentropic compression. The effectiveness *e* between the suction gas and the [isothermal] metal parts is assumed to be constant over the range of mass flow rates and is determined by minimizing the following objective function to obtain the best agreement with the measured mass flow rate at *N* data points.

$$obj\_F = \min \sqrt{\frac{\sum_{n=1}^{N} \left(\frac{F_{\exp} - F_{cal}}{F_{\exp}} \right)^2}{N}} \tag{6}$$

The objective function (*F*) is mass flow rate (*m*), power consumption (*W*), or discharge temperature (T_{dis}).

The compressor power consumption can be calculated if the compressor efficiency is known. The isentropic compressor efficiency is normally defined across the entire compressor shell, but in our case we define a compression efficiency that excludes the effects of subsystem heat transfers upstream of the suction port, and includes the effects of motor efficiency:

$$h_c = \dot{m}[h(P_{dp}, s_{sp}) - h_{sp}]/W \tag{7}$$

Kim and Bullard [1] extracted the linear relationship between the isentropic compressor efficiency and the shell temperature from large data sets. As shown in Figs. 6 and 7, the compressor efficiency can be presented also as a function of the pressure ratio as well as the shell temperature:

$$h_c = k_1 + k_2 \frac{P_{dis}}{P_{suc}} \tag{8}$$

$$h_c = k_3 + k_4 T_{shell} \tag{9}$$

where the constants k_1 and k_2 can be determined directly from Eqs. (7) and (8), but when we use the compressor efficiency Eq. (9), the associated two constants k_3 and k_4 should be estimated by minimizing the average normalized deviation between the measured and calculated power consumptions from Eq. (6).

The empirically observed dependence of compression efficiency on discharge (hence indirectly on shell) temperature is thought to reflect the temperature dependence of oil viscosity. The principal mechanism of oil cooling, splattering onto the compressor shell, determines the relationship between shell temperature and oil temperature.

Three more parameters are needed to estimate the discharge temperature. The first step is to apply the first law of thermodynamics across the compressor shell using the following equation for the steady state flow, neglecting the potential and kinetic energy.

$$Q = W - \dot{m}(h_{dis} - h_{suc}) \qquad (10)$$

The previous experimental observations [1] suggested a linear relationship with the discharge temperature as shown in Fig. 7

$$T_{shell} = a + bT_{dis} \qquad (11)$$

where a and b are empirical constants determined from at least two experimental data points.

Finally, the heat transfer from the compressor shell can be obtained from the equation

$$Q = UA_{shell}(T_{shell} - T_{amb}) \qquad (12)$$

If discharge temperatures are available for more operating conditions, UA_{shell} is a constant to be determined using the least squares method with the measured discharge temperatures from Eq. (6)

A Newton-Raphson based equation solver [18] was used for both the simulation and optimization calculations needed to estimate these parameters.

4. Simulation and parameter estimation results

Table 1 shows the compressor data sets used in this study: the compressor geometry (displacement and clearance volume ratio), refrigerant and number of data points. Three refrigerant (R-22 and its alternative R-410A and R-407C) compressors are considered: three compressors for each refrigerant. Appendix A presents all the data sets and they are collected over a wide range of operating conditions: evaporating temperature (-10 - 10°C), condensing temperature (40 - 60°C), suction temperature (4 - 37°C) and ambient temperature (20 - 40°C).

Table 1. Data sets used for computer simulations

Data set	Refrigerant	Compressor model	Displacement (cc)	Clearance volume ratio (%)	Compressor speed (rpm)	Data points, N
I-1	R-22	44A072I	10.32	1.8	3450	44
I-2		44B092J	16.08	1.7	2850	35
I-3		44B124I	17.64	1.5	3500	40
II-1	R-410A	G4A080J	10.32	1.8	2850	40
II-2		G4B102J	13.22	2.1	2850	40
II-3		G8B120J	15.02	3.9	2850	40
III-1	R-407C	F4B080J	14.06	1.9	2850	40
III-2		F4B092J	16.08	1.7	2850	105
III-3		F8B145J	25.04	2.4	2850	41

The simulation results are depicted in Figs. 4–10 and Table 2 shows the estimated parameters and RMS errors of simulation results for each data set. The parameter estimates were obtained using the complete data sets. The small standard deviations apparent from Figs. 4-10 suggest that smaller subsets of data could yield similar results. The overall calculation results are in good agreement with measured data within a reasonable accuracy as shown in Table 2: the RMS errors for calculated mass flow rates and power inputs are within 2.7% and 2.8%, especially considering measurement accuracy, and the difference between the calculated and measured discharge temperatures is below 2.8°C.

Table 2. Estimated parameters and RMS errors

Data set	Estimated constants							RMS errors		
								%		°C
	a	*e*	k_1	k_2 x10^2	*a*	*b*	UA_{shell}	*obj_mr*	*obj_W*	DT_{dis}
I-1	1.099	0.3863	0.787	-1.083	-4.995	1.037	3.813	2.1	1.8	1.1
I-2	1.126	0.4038	0.783	-1.131	-7.506	1.073	4.253	1.2	1.6	1.3
I-3	1.060	0.3580	0.709	+0.325	-3.443	0.954	4.493	1.3	2.3	1.5
II-1	1.208	0.5164	0.861	-1.470	-2.278	1.011	3.898	1.9	2.2	2.4
II-2	1.278	0.5778	0.899	-2.038	-6.391	1.039	3.919	2.5	2.4	2.0
II-3	1.266	0.5269	0.967	-7.199	-10.07	1.073	4.426	2.7	1.4	2.8
III-1	1.213	0.4998	0.816	-1.491	-7.849	1.063	4.086	2.5	2.8	1.7
III-2	1.113	0.3927	0.729	-0.468	-5.549	1.030	4.811	1.8	2.2	2.2
III-3	1.093	0.267	0.740	-1.757	-2.982	0.989	4.944	1.0	2.3	1.8

Figure 4 presents the clearance volumetric efficiency as a function of pressure ratio. As expected, the clearance volumetric efficiency for the rotary compressors decreases systematically as the pressure ratio and clearance volume increases. It varies from 0.89 to 0.98, depending on the individual design and the operating conditions and has a relatively higher value compared to the reciprocating compressors (0.60-0.90) since the clearance volume and the associated re-expansion of the clearance gas are small. However, for data set II-3, the clearance volumetric efficiency (0.66-0.92) is smaller than the compressors because its clearance volume ratio (3.9%) is larger than the others (1.5-2.4 %) as shown in Table 2. Figure 5 presents a comparison of the calculated and measured mass flow rates and they are in excellent agreement over a whole range of test conditions.

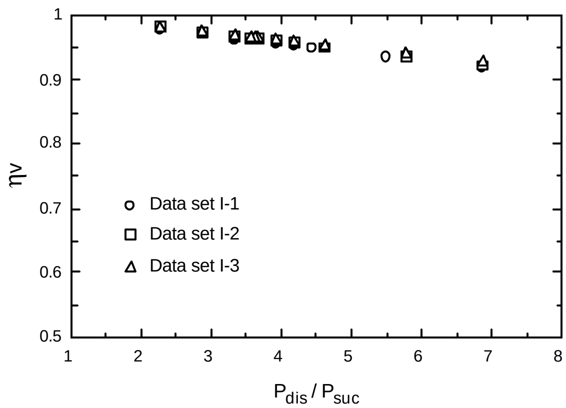

Figure 4(a). R-22

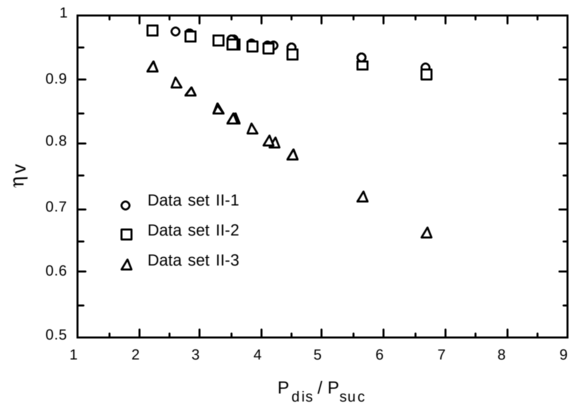

Figure 4(b). R-410A

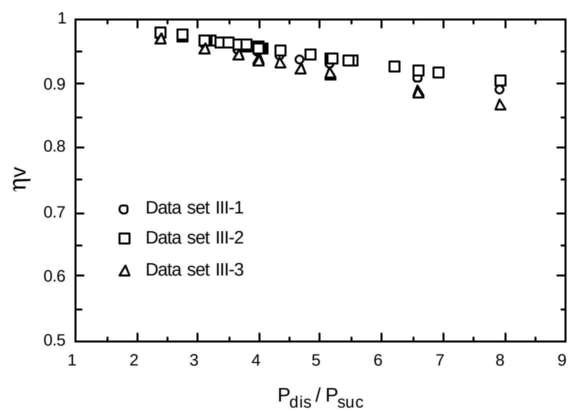

Figure 4(c). R-407C

Figure 4. Clearance volumetric efficiency as a function of a pressure ratio

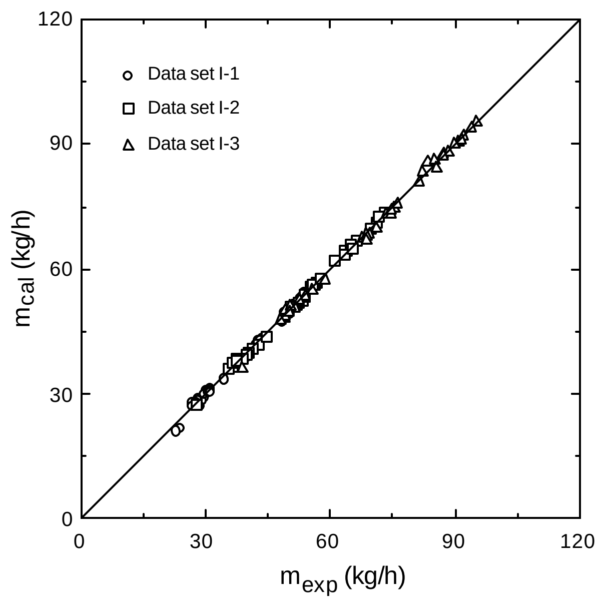

Figure 5(a). R-22

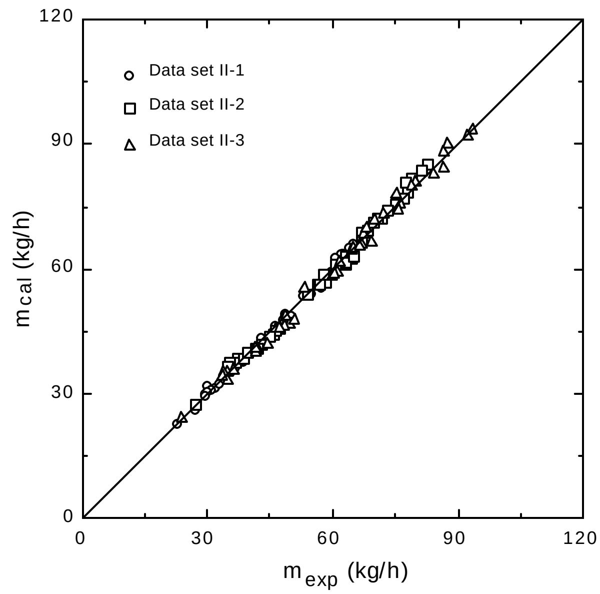

Figure 5(b). R-410A

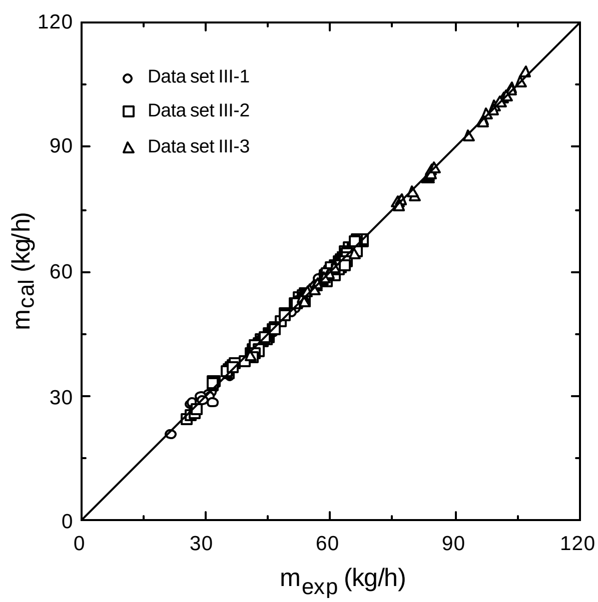

Figure 5(c). R-407C

Figure 5. Refrigerant mass flow rate

Figures 6-8 present the results of power consumption submodel. Figures 6 and 7 depict isentropic compressor efficiencies as functions of shell temperature and pressure ratio, respectively. Pre-calculation results indicated that the accuracy of the calculated power consumption associated with Eq. (8) was better than with Eq. (9), so Eq. (8) was used for the all the calculations. As described earlier, when we use Eq. (8) for the compressor efficiency, the associated coefficients (k_1 and k_2) are determined directly from Eqs. (7) and (8) using the results of the mass flow submodel. Figure 8 shows compressor power consumption and the calculated compressor powers are in good agreement with measured values within 2.8%.

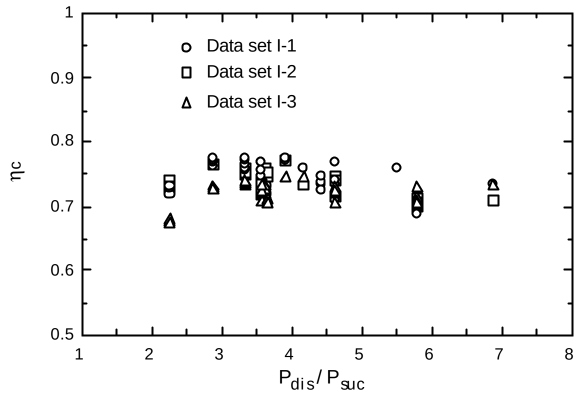

Figure 6(a). R-22

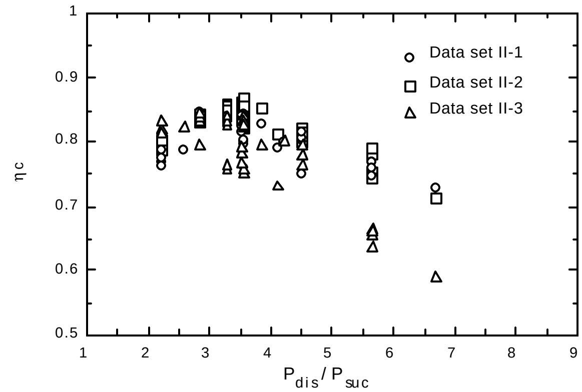

Figure 6(b). R-410A

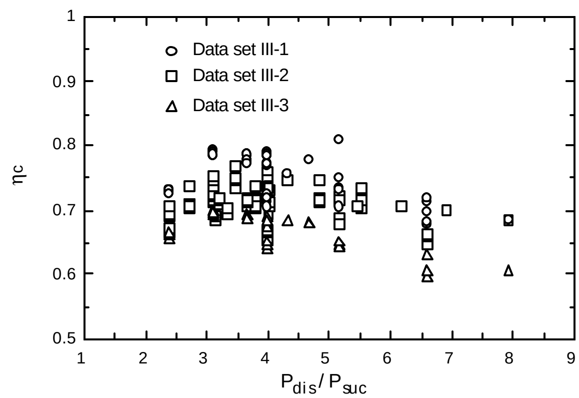

Figure 6(c). R-407C

Figure 6. Isentropic compressor efficiency as a function of pressure ratio

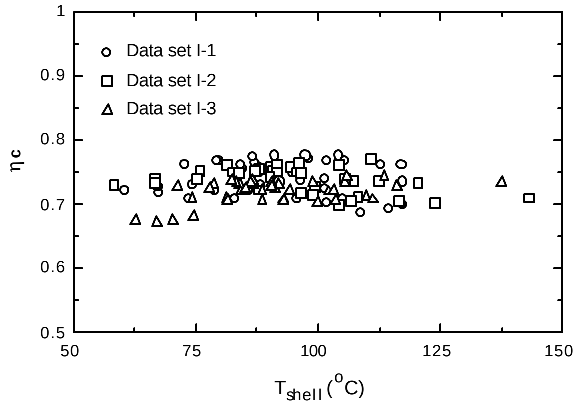

Figure 7(a). R-22

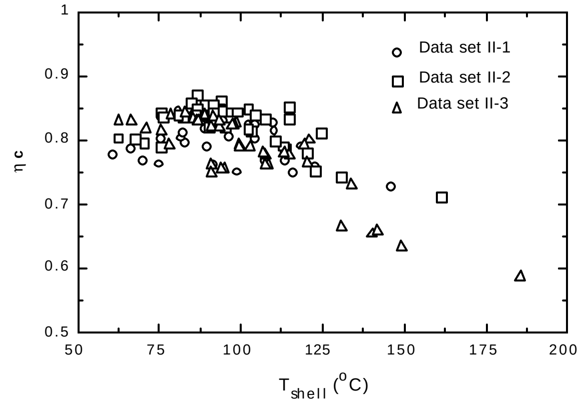

Figure 7(b). R-410A

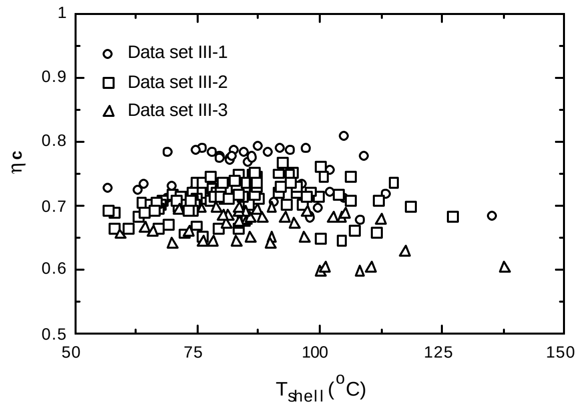

Figure 7(c). R-407C

Figure 7. Isentropic compressor efficiency as a function of shell temperature

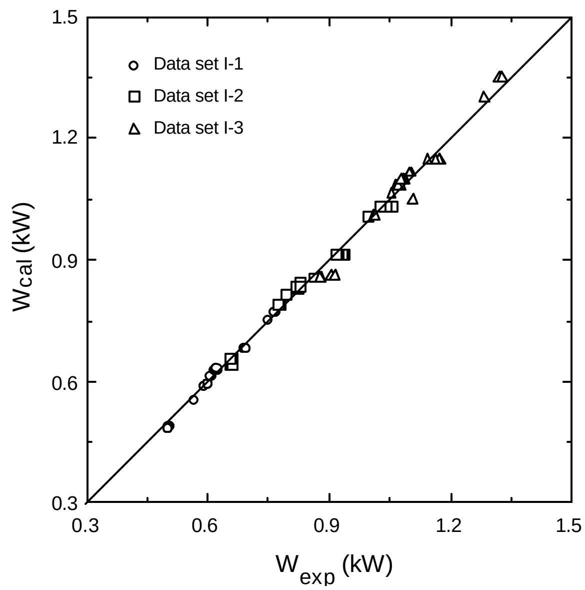

Figure 8(a). R-22

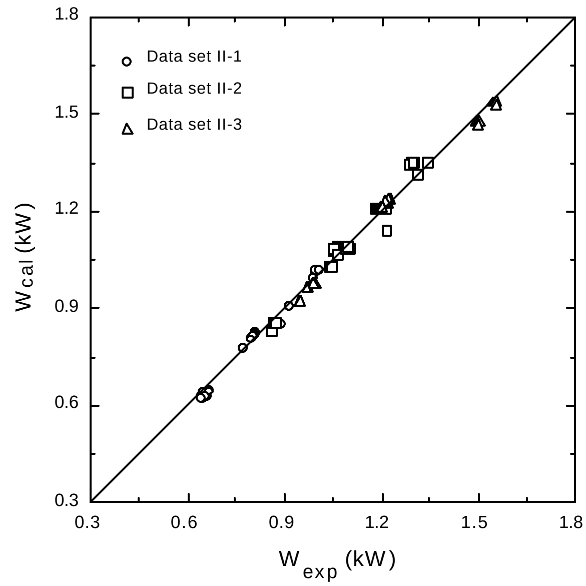

Figure 8(b). R-410A

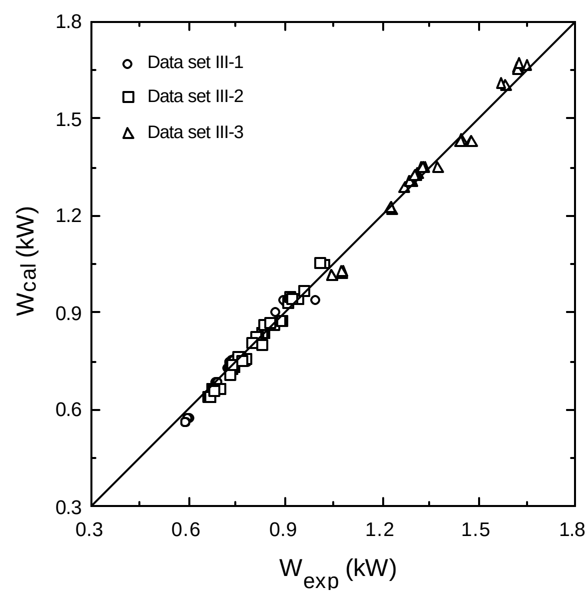

Figure 8(c). R-407C

Figure 8. Compressor power consumption

Figure 9 demonstrates the linearity of the empirical correlation between the compressor shell and discharge temperatures. This relation is used for estimating the discharge temperature and the overall heat transfer coefficient, UA_{shell}, of the compressor shell. Figure 10 shows a comparison of the calculated and measured discharge temperatures.

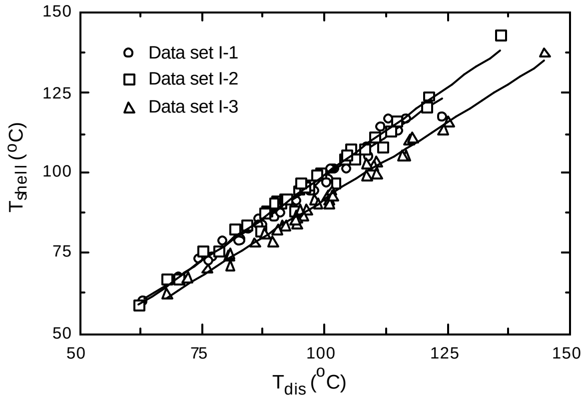

Figure 9(a). R-22

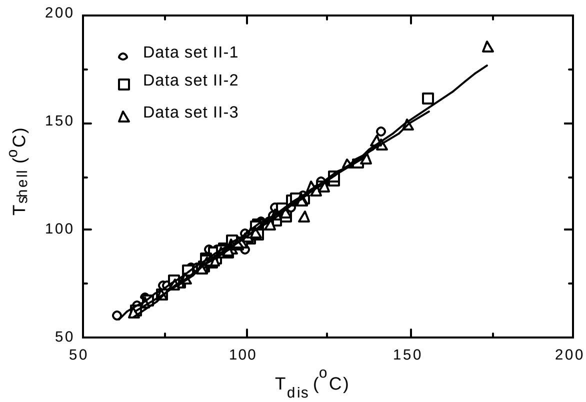

Figure 9(b). R-410A

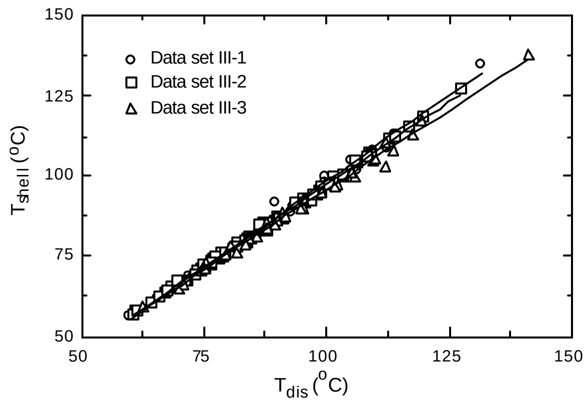

Figure 9(c). R-407C

Figure 9. Compressor shell temperature vs. discharge temperature

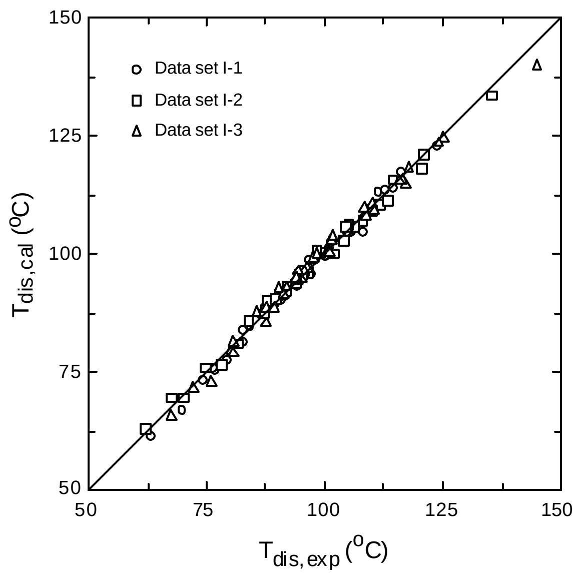

Figure 10(a). R-22

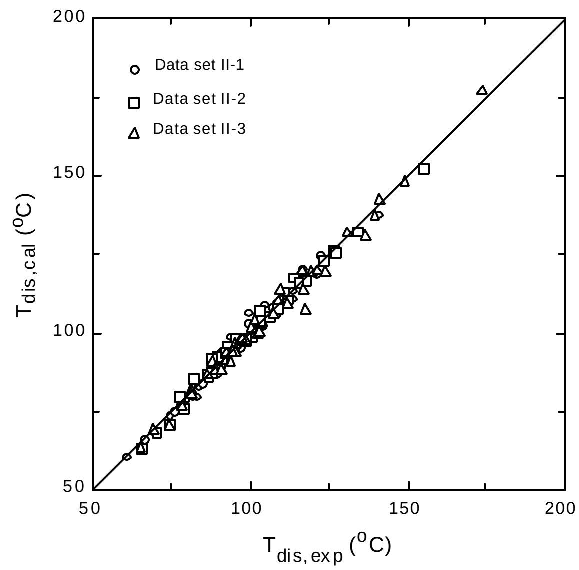

Figure 10(b). R-410A

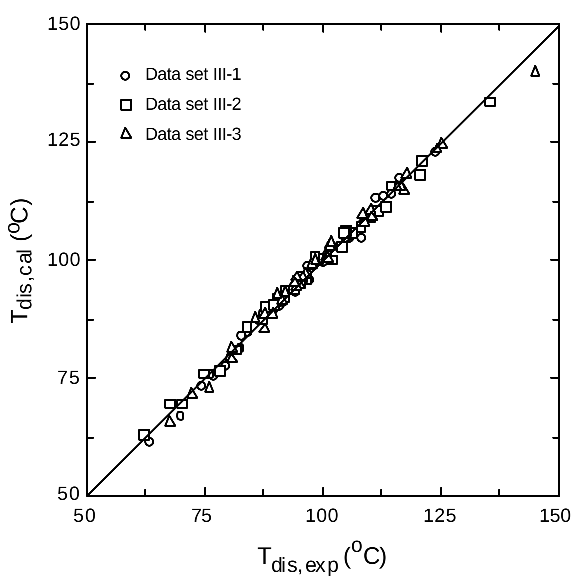

Figure 10(c). R-407C

Figure 10. Compressor discharge temperature

5. Conclusions

A simple and general compressor model developed using the thermodynamic principles and large data sets from the compressor calorimeter and *in-situ* tests has been successfully applied to the different type of the high-side sump rolling-piston-type rotary compressors. The model can estimate mass flow rate/compressor power consumption and discharge temperature with rms errors less than 3% and 2.8°C, respectively, which is not much larger than measurement errors associated with calorimeter testing under ideal conditions. The magnitude of the errors suggests that the seven parameters could be estimated from data sets much smaller than those used here. The density decrease due to suction gas heating and mixing is a very important factor affecting mass flow rate. Oil viscosity appears to be the most important factor accounting for compressor power consumption more than the isentropic ideal.

Fewer tests should be needed in calorimeter to estimate these seven physical parameters, compared to the 18-20 parameters needed for today's polynomial curve fits of mass flow and power. However this approach requires that T_{shell} and T_{dis} should be recorded for at least two operating conditions during the calorimeter tests, in order to define the simple linear relation between them and to estimate the compressor shell heat transfer coefficient. Similarly, only two such data points would need to be obtained by OEM's to characterize accurately the compressor shell heat transfer coefficient in unique installations, where the air temperature at the compressor is influenced by the location of the condenser.

6. References

1. Kim, Man-Hoe and Bullard, Clark W., 2001, "A Simple Approach on the Thermal Performance Analysis of Small Hermetic Reciprocating Compressors," ASHRAE Trans. Vol. 107, Pt. 1.
2. Srichai, P.R. and Bullard, C.W. 1997. Two-speed compressor operation in a refrigerator/freezer. ACRC TR-121. University of Illinois at Urbana-Champaign.
3. Kelman, S. and Bullard, C.W. 1999. Dual temperature evaporator refrigerator design and optimization. ACRC TR-148. University of Illinois at Urbana-Champaign.
4. Dabiri, A.E. and Rice, C.K., 1981, "A compressor simulation model with corrections for the level of suction gas superheat," ASHRAE Transactions Vol. 87, Pt. 2, pp. 771-782.
5. Mullen, C.E., Bridges, B.D, Porter, K.J., Hahn, G.W. and Bullard, C.W. 1998, "Development and validation of a room air conditioning simulation model," ASHRAE Transactions Vol. 104, Pt. 2, pp. 389-397.
6. Haider, I., Lavannis, M.K. and Radermacher, R., 1997, "Investigations of the EPA refrigerator analysis (ERA) software: compressor map and ambient temperature effects," ASHRAE Transactions, Vol. 103, Pt. 11, pp. 608-618.
7. Prakash, R. and Singh, R., 1974, "Mathematical modeling and simulation of refrigerating compressors," Proceedings of the 1974 Purdue Compressor Technology Conference, pp. 274-285.
8. Hiller, C.C. and Glicksman, L.R., 1976, "Detailed modeling and computer simulation of reciprocating refrigeration compressors," Proceedings of the 1976 Purdue Compressor Technology Conference, pp. 12-17.
9. Domanski, P.A. and Didion, D.A., 1983, "Computer modeling of the vapor compression cycle with constant flow area expansion device," National Bureau of Standards, Building Science Series No. 155.
10. Todescat, M.L., Fagotti, F., Prata, A.T. and Ferrerira, R.T.S., 1992, "Thermal energy analysis in reciprocating hermetic compressors," Proceedings of the 1992 International Compressor Engineering Conference at Purdue, pp. 1419-1428.
11. Cavallini, A., Doretti, L., Longo, G.A., Rossetto, L., Bella, B., and Zannerio, A., 1996, "Thermal analysis of a hermetic reciprocating compressor," Proceedings of the 1996 International Compressor Conference, Purdue University, West Lafayette, Indiana, pp. 535-540.
12. Rigola, J., Perez-Segarra, C.D., Oliva, A., Serra, J.M., Escriba, M. and Pons, J., 1996, "Parametric study and experimental comparison of small hermetic refrigeration compressors using an advanced numerical simulation model," Proceedings of the 1996 International Compressor Engineering Conference at Purdue, pp. 529-534.
13. Jahnig, D.I., Reindl, D.T. and Klein, S.A., 2000, "A semi-empirical method for representing domestic refrigerator/freezer compressor calorimeter test data," ASHRAE Trans. Vol. 106, Pt. 2.
14. Dossat, R.Y., Principles of Refrigeration, 2nd edition, John Wiley & Sons, 1981.
15. Kuehn, T.M., Ramsey, J.W. and Threlkeld, J.L., 1998, Thermal environmental engineering, 3rd edition, Prentice Hall.
16. ASHRAE, 2000, ASHRAE Handbook- HVAC System and Equipment, pp.34.1-34.36.
17. Rasmussen, B.D., 1997, "Variable speed hermetic reciprocating compressors for domestic refrigerators," Ph.D. Thesis, Technical University of Denmark.
18. Klein, S.A. and Alvarado, F.L., 2000, Engineering equation solver, F-Chart Software.
19. Shigley, J.E. and Mitchell, L.D., Mechanical Engineering Design, 4th edition, McGraw-Hill Book Company, 1983.

Appendix A. Data sets used for the model and simulation results

A-1 Data set I-1

T_{evap} (°C)	T_{cond} (°C)	T_{suc} (°C)	T_{shell} (°C)	T_{amb} (°C)	$T_{dis,exp}$ (°C)	$T_{dis,cal}$ (°C)	$m_{r,exp}$ (kg/h)	$m_{r,cal}$ (kg/h)	W_{exp} (kW)	W_{cal} (kW)	h_v	h_c
-10.0	50.0	36.8	117.1	35.0	112.8	113.6	23.59	22.19	0.567	0.559	0.94	0.73
-10.0	60.0	30.5	117.5	35.0	123.8	123.3	22.85	21.50	0.657	0.640	0.92	0.71
-5.0	40.0	8.1	73.7	20.0	74.3	73.4	31.09	31.82	0.506	0.492	0.96	0.75
-5.0	40.0	15.0	79.1	20.0	79.3	77.7	30.65	31.01	0.504	0.492	0.96	0.75
-5.0	40.0	15.6	82.9	40.0	84.1	84.9	30.24	30.94	0.505	0.492	0.96	0.75
-5.0	40.0	22.7	88.3	40.0	89.3	89.4	30.10	30.16	0.502	0.492	0.96	0.75
-5.0	50.0	8.5	85.9	20.0	86.7	87.3	29.63	30.24	0.591	0.590	0.95	0.74
-5.0	50.0	15.0	90.9	20.0	90.9	91.4	29.46	29.54	0.588	0.590	0.95	0.74
-5.0	50.0	16.2	95.9	40.0	96.7	98.9	28.38	29.41	0.589	0.590	0.95	0.74
-5.0	50.0	22.9	101.4	40.0	101.7	103.2	28.89	28.74	0.589	0.590	0.95	0.74
-5.0	50.0	36.9	110.9	35.0	110.0	110.0	28.60	27.44	0.589	0.590	0.95	0.74
-5.0	60.0	8.9	101.7	20.0	101.1	101.5	28.24	28.70	0.693	0.684	0.93	0.72
-5.0	60.0	15.0	108.8	20.0	108.5	105.2	27.04	28.10	0.691	0.684	0.93	0.72
-5.0	60.0	15.5	105.0	20.0	105.6	105.5	27.78	28.05	0.692	0.684	0.93	0.72
-5.0	60.0	17.0	114.4	40.0	111.5	113.3	27.09	27.91	0.692	0.684	0.93	0.72
-5.0	60.0	23.5	117.4	40.0	116.3	117.3	26.79	27.31	0.693	0.684	0.93	0.72
-3.8	50.0	16.6	92.1	20.0	91.7	91.3	31.00	30.87	0.600	0.596	0.95	0.74
-3.8	50.0	20.5	96.4	30.0	96.8	97.0	30.54	30.45	0.598	0.596	0.95	0.74
-3.8	50.0	20.7	96.2	30.0	96.7	97.2	30.91	30.43	0.596	0.596	0.95	0.74
-3.8	50.0	23.9	101.5	40.0	101.5	102.6	29.73	30.09	0.598	0.596	0.95	0.74
0.0	50.0	36.5	104.6	35.0	105.8	105.1	34.62	33.70	0.608	0.614	0.96	0.74
0.0	50.0	36.7	104.2	35.0	105.6	105.2	34.66	33.68	0.605	0.614	0.96	0.74
5.0	50.0	19.6	84.5	40.0	87.2	89.0	43.30	43.64	0.618	0.628	0.97	0.75
5.0	50.0	20.7	84.2	30.0	86.7	87.2	43.41	43.46	0.618	0.628	0.97	0.75
5.0	50.0	23.2	87.8	40.0	90.3	91.6	42.86	43.05	0.618	0.628	0.97	0.75
5.0	50.0	24.2	87.2	30.0	89.6	89.6	43.10	42.89	0.618	0.628	0.97	0.75
5.0	50.0	27.1	91.3	40.0	93.7	94.4	42.43	42.43	0.619	0.628	0.97	0.75
5.0	50.0	36.4	98.3	35.0	100.5	99.6	41.75	41.04	0.621	0.629	0.97	0.75
5.0	50.0	36.5	97.6	35.0	100.1	99.6	41.57	41.02	0.616	0.629	0.97	0.75
5.0	60.0	36.5	112.9	35.0	114.8	114.0	39.92	39.26	0.746	0.753	0.95	0.74
10.0	40.0	17.3	60.7	20.0	63.1	61.4	55.40	56.03	0.503	0.484	0.98	0.76
10.0	40.0	22.4	67.7	40.0	70.1	69.7	53.78	54.82	0.503	0.484	0.98	0.76
10.0	40.0	24.8	67.4	20.0	69.7	67.0	53.78	54.27	0.501	0.484	0.98	0.76
10.0	40.0	30.2	74.3	40.0	76.9	75.6	52.75	53.09	0.500	0.484	0.98	0.76
10.0	50.0	17.4	72.9	20.0	76.2	76.0	53.20	53.49	0.621	0.632	0.97	0.76
10.0	50.0	22.4	79.9	40.0	82.8	84.2	52.28	52.40	0.619	0.632	0.97	0.76
10.0	50.0	24.9	79.3	20.0	82.6	81.6	51.85	51.88	0.620	0.632	0.97	0.76
10.0	50.0	30.1	86.6	40.0	89.6	90.0	50.98	50.84	0.619	0.633	0.97	0.76
10.0	50.0	36.2	91.4	35.0	94.2	93.4	50.37	49.68	0.624	0.633	0.97	0.76
10.0	60.0	17.4	88.0	20.0	90.9	90.8	50.77	51.08	0.767	0.774	0.96	0.75
10.0	60.0	22.7	94.9	40.0	98.0	99.1	49.32	50.03	0.761	0.775	0.96	0.75
10.0	60.0	24.8	94.6	20.0	97.2	96.1	49.88	49.63	0.769	0.775	0.96	0.75
10.0	60.0	30.2	101.7	40.0	104.6	104.7	49.34	48.64	0.764	0.775	0.96	0.75
10.0	60.0	36.4	105.6	35.0	108.7	108.1	48.17	47.55	0.762	0.775	0.96	0.75

A-2 Data set I-2

T_{evap} (°C)	T_{cond} (°C)	T_{suc} (°C)	T_{shell} (°C)	T_{amb} (°C)	$T_{dis,exp}$ (°C)	$T_{dis,cal}$ (°C)	$m_{r,exp}$ (kg/h)	$m_{r,cal}$ (kg/h)	W_{exp} (kW)	W_{cal} (kW)	h_v	h_c
-10.0	60.0	36.7	143	35.0	135.7	133.7	27.91	27.42	0.866	0.855	0.92	0.71
-5.0	40.0	6.6	75.85	20.0	75.0	75.8	42.50	41.71	0.659	0.656	0.96	0.74
-5.0	40.0	12.7	84.05	40.0	83.9	86.0	41.06	40.78	0.656	0.656	0.96	0.74
-5.0	40.0	14.1	82.5	20.0	81.4	80.9	41.19	40.57	0.657	0.656	0.96	0.74
-5.0	40.0	20.3	90.8	40.0	90.2	91.1	40.22	39.68	0.654	0.656	0.96	0.74
-5.0	50.0	6.9	90.35	20.0	89.7	90.7	39.94	39.57	0.780	0.787	0.95	0.73
-5.0	50.0	12.8	98.75	40.0	98.2	100.7	37.61	38.74	0.779	0.787	0.95	0.73
-5.0	50.0	14.2	96.5	20.0	95.3	95.5	39.00	38.55	0.777	0.787	0.95	0.73
-5.0	50.0	20.4	105.4	40.0	104.4	105.8	37.64	37.74	0.775	0.786	0.95	0.73
-5.0	60.0	6.9	104.1	20.0	106.0	105.7	37.54	37.54	0.937	0.913	0.94	0.72
-5.0	60.0	7.4	106.9	20.0	105.2	106.0	36.83	37.47	0.914	0.913	0.94	0.72
-5.0	60.0	13.3	116.3	40.0	114.5	115.9	36.30	36.72	0.920	0.913	0.94	0.72
-5.0	60.0	14.4	108.3	20.0	111.7	110.5	37.09	36.58	0.932	0.913	0.94	0.72
-5.0	60.0	21.1	123.6	40.0	121.2	121.1	35.45	35.78	0.924	0.913	0.94	0.72
0.0	50.0	36.6	110.9	35.0	110.2	109.2	44.66	43.93	0.796	0.817	0.96	0.74
2.5	50.0	15.3	81.65	20.0	86.8	87.2	53.31	52.36	0.824	0.828	0.96	0.74
2.5	50.0	18.0	90.6	30.0	90.7	91.6	52.16	51.84	0.818	0.828	0.96	0.74
2.5	50.0	20.3	94.45	40.0	94.5	95.7	51.99	51.40	0.822	0.829	0.96	0.74
5.0	50.0	17.4	87.2	40.0	87.9	89.9	57.44	57.41	0.827	0.836	0.97	0.74
5.0	50.0	19.5	87.75	30.0	88.3	89.2	56.81	56.95	0.822	0.836	0.97	0.74
5.0	50.0	21.9	91.4	40.0	92.1	93.3	55.69	56.43	0.819	0.837	0.97	0.74
5.0	50.0	23.5	91.4	30.0	91.8	92.2	56.18	56.10	0.820	0.837	0.97	0.74
5.0	50.0	26.0	95.45	40.0	95.8	96.4	55.07	55.58	0.823	0.837	0.97	0.74
5.0	50.0	36.2	104	35.0	104.0	102.7	53.69	53.60	0.822	0.837	0.97	0.74
5.0	60.0	36.6	120.4	35.0	120.6	118.2	50.47	51.14	0.996	1.004	0.96	0.74
10.0	40.0	16.7	58.35	20.0	62.0	62.7	73.03	73.48	0.662	0.644	0.98	0.76
10.0	40.0	20.3	66.65	40.0	67.6	69.4	71.73	72.35	0.660	0.644	0.98	0.76
10.0	40.0	25.2	66.65	20.0	70.3	69.4	71.00	70.89	0.660	0.644	0.98	0.76
10.0	40.0	29.1	75.2	40.0	78.3	76.4	69.56	69.78	0.656	0.644	0.98	0.76
10.0	50.0	36.4	96.05	35.0	96.8	96.1	65.19	64.86	0.829	0.842	0.97	0.75
10.0	60.0	17.0	87.85	20.0	93.8	93.6	66.47	66.66	1.057	1.031	0.96	0.74
10.0	60.0	20.7	99.45	40.0	99.1	100.3	64.91	65.70	1.041	1.032	0.96	0.74
10.0	60.0	25.3	96.4	20.0	102.1	99.9	63.78	64.57	1.054	1.032	0.96	0.74
10.0	60.0	29.5	107.1	40.0	108.0	107.1	63.29	63.57	1.036	1.032	0.96	0.74
10.0	60.0	36.3	112.5	35.0	113.3	111.3	60.97	62.04	1.026	1.033	0.96	0.74

A-3 Data set I-3

T_{evap} (°C)	T_{cond} (°C)	T_{suc} (°C)	T_{shell} (°C)	T_{amb} (°C)	$T_{dis,exp}$ (°C)	$T_{dis,cal}$ (°C)	$m_{r,exp}$ (kg/h)	$m_{r,cal}$ (kg/h)	W_{exp} (kW)	W_{cal} (kW)	h_v	h_c
-10.0	60.0	37.2	137.3	35.0	144.8	140.4	38.53	36.57	1.104	1.055	0.93	0.73
-5.0	40.0	5.9	74.3	20.0	80.1	79.8	55.46	55.00	0.876	0.858	0.97	0.72
-5.0	40.0	10.8	81.6	40.0	87.5	88.8	53.89	53.97	0.875	0.858	0.97	0.72
-5.0	40.0	13.7	81.1	20.0	87.5	85.7	53.98	53.38	0.878	0.858	0.97	0.72
-5.0	40.0	18.8	88.6	40.0	94.8	95.0	52.47	52.38	0.875	0.858	0.97	0.72
-5.0	50.0	6.1	84.2	20.0	94.2	94.7	52.40	52.57	1.010	1.011	0.95	0.72
-5.0	50.0	11.5	93.0	40.0	101.6	104.1	50.26	51.52	1.009	1.011	0.95	0.72
-5.0	50.0	14.0	90.5	20.0	100.9	100.6	51.67	51.06	1.014	1.011	0.95	0.72
-5.0	50.0	19.3	103.1	40.0	108.4	110.1	50.13	50.10	1.011	1.011	0.95	0.72
-5.0	60.0	6.5	99.9	20.0	110.5	109.4	49.24	50.16	1.163	1.149	0.94	0.73
-5.0	60.0	6.6	103.5	20.0	110.5	109.5	49.72	50.14	1.172	1.149	0.94	0.73
-5.0	60.0	11.6	111.2	40.0	117.8	118.6	48.93	49.24	1.170	1.149	0.94	0.73
-5.0	60.0	14.2	109.9	20.0	117.0	115.1	48.76	48.80	1.171	1.149	0.94	0.73
-5.0	60.0	19.7	116.1	40.0	125.2	124.7	47.72	47.87	1.142	1.149	0.94	0.73
0.0	50.0	36.9	105.8	35.0	115.9	115.7	58.93	57.69	1.052	1.065	0.96	0.72
2.5	50.0	15.3	84.0	20.0	91.2	91.7	69.33	68.87	1.073	1.085	0.97	0.72
2.5	50.0	17.3	86.9	30.0	94.1	95.4	68.45	68.34	1.067	1.085	0.97	0.72
2.5	50.0	17.3	86.5	30.0	94.1	95.4	68.50	68.34	1.069	1.085	0.97	0.72
2.5	50.0	19.5	91.4	40.0	97.8	99.4	67.75	67.76	1.076	1.085	0.97	0.72
5.0	50.0	16.7	82.2	40.0	90.3	93.1	76.02	75.55	1.077	1.101	0.97	0.72
5.0	50.0	19.2	83.3	30.0	91.9	93.2	75.22	74.81	1.082	1.101	0.97	0.72
5.0	50.0	20.8	86.1	40.0	94.2	96.5	74.44	74.34	1.077	1.101	0.97	0.72
5.0	50.0	23.3	86.6	30.0	95.6	96.6	74.39	73.63	1.082	1.101	0.97	0.72
5.0	50.0	25.2	90.5	40.0	98.4	100.2	73.44	73.10	1.082	1.101	0.97	0.72
5.0	50.0	36.5	98.9	35.0	108.6	108.4	70.91	70.12	1.087	1.101	0.97	0.72
5.0	60.0	36.7	113.4	35.0	124.0	123.8	68.38	67.38	1.281	1.301	0.96	0.72
10.0	40.0	16.7	62.6	20.0	67.5	65.8	95.14	95.48	0.910	0.864	0.98	0.72
10.0	40.0	19.7	67.1	40.0	72.0	71.7	93.64	94.22	0.913	0.864	0.98	0.72
10.0	40.0	25.2	70.2	20.0	75.9	73.0	91.70	92.02	0.910	0.864	0.98	0.72
10.0	40.0	28.5	74.7	40.0	80.4	79.3	90.63	90.77	0.905	0.864	0.98	0.72
10.0	50.0	16.7	71.3	20.0	80.7	81.5	91.35	91.60	1.096	1.116	0.98	0.72
10.0	50.0	20.2	78.1	40.0	85.7	87.9	89.95	90.26	1.097	1.117	0.98	0.72
10.0	50.0	25.4	78.6	20.0	89.1	88.9	88.33	88.35	1.096	1.117	0.98	0.72
10.0	50.0	28.7	85.3	40.0	93.9	95.2	86.98	87.20	1.099	1.117	0.98	0.72
10.0	50.0	36.4	91.7	35.0	100.8	100.8	85.25	84.64	1.103	1.118	0.98	0.72
10.0	60.0	16.8	88.6	20.0	96.3	97.2	86.82	87.86	1.327	1.351	0.97	0.72
10.0	60.0	20.2	94.3	40.0	101.3	103.5	85.09	86.65	1.319	1.351	0.97	0.72
10.0	60.0	21.2	92.8	20.0	100.6	100.9	83.53	86.31	1.326	1.351	0.97	0.72
10.0	60.0	28.8	102.1	40.0	109.9	110.8	82.18	83.79	1.324	1.352	0.97	0.72
10.0	60.0	36.3	105.4	35.0	116.3	116.2	81.48	81.48	1.326	1.353	0.97	0.72

A-4 Data set II-1

T_{evap} (°C)	T_{cond} (°C)	T_{suc} (°C)	T_{shell} (°C)	T_{amb} (°C)	$T_{dis,exp}$ (°C)	$T_{dis,cal}$ (°C)	$m_{r,exp}$ (kg/h)	$m_{r,cal}$ (kg/h)	W_{exp} (kW)	W_{cal} (kW)	h_v	h_c
-10.0	40.0	36.6	111.0	35.0	108.9	106.0	26.93	26.27	0.642	0.626	0.95	0.80
-10.0	60.0	36.7	146.0	35.0	141.3	137.6	22.92	22.89	0.894	0.855	0.92	0.76
-5.0	40.0	6.6	75.3	20.0	76.1	74.7	36.63	36.44	0.653	0.646	0.96	0.81
-5.0	40.0	11.7	83.1	40.0	83.6	83.4	35.66	35.72	0.654	0.646	0.96	0.81
-5.0	40.0	14.0	82.0	20.0	82.3	80.1	35.64	35.40	0.653	0.646	0.96	0.81
-5.0	40.0	19.1	91.7	40.0	91.3	88.9	33.90	34.73	0.668	0.646	0.96	0.81
-5.0	50.0	10.4	89.5	20.0	90.7	93.2	34.16	33.46	0.771	0.778	0.95	0.79
-5.0	50.0	16.0	96.2	20.0	96.9	97.2	33.04	32.79	0.771	0.778	0.95	0.79
-5.0	50.0	21.2	98.8	40.0	99.9	106.2	30.24	32.20	0.771	0.778	0.95	0.79
-5.0	50.0	25.1	104.3	40.0	104.9	109.0	31.98	31.77	0.775	0.778	0.95	0.79
-5.0	60.0	10.4	107.5	20.0	108.5	109.6	30.97	31.16	0.912	0.908	0.93	0.78
-5.0	60.0	16.0	113.6	20.0	114.1	113.6	30.39	30.57	0.913	0.908	0.93	0.78
-5.0	60.0	18.1	116.3	40.0	117.1	120.4	29.43	30.35	0.914	0.908	0.93	0.78
-5.0	60.0	23.9	122.8	40.0	123.1	124.5	29.36	29.78	0.918	0.909	0.93	0.78
0.0	50.0	36.4	109.6	35.0	111.0	109.2	38.57	37.88	0.798	0.807	0.96	0.80
2.5	50.0	16.4	85.6	20.0	87.6	87.3	45.83	45.26	0.800	0.816	0.96	0.81
2.5	50.0	21.3	88.9	30.0	90.8	93.1	45.43	44.39	0.802	0.816	0.96	0.81
2.5	50.0	25.8	92.3	40.0	94.1	98.7	44.80	43.64	0.803	0.816	0.96	0.81
5.0	40.0	36.3	89.8	35.0	89.6	86.6	48.88	49.60	0.667	0.651	0.98	0.82
5.0	50.0	21.2	86.0	40.0	88.0	91.2	50.24	49.29	0.807	0.823	0.97	0.81
5.0	50.0	21.4	91.4	30.0	88.7	89.5	49.65	49.25	0.806	0.823	0.97	0.81
5.0	50.0	24.7	90.0	30.0	92.2	92.1	48.80	48.61	0.807	0.823	0.97	0.81
5.0	50.0	24.7	89.7	40.0	91.7	94.0	49.15	48.61	0.807	0.823	0.97	0.81
5.0	50.0	28.1	93.1	40.0	95.4	96.7	48.14	47.98	0.808	0.823	0.97	0.81
5.0	50.0	36.5	102.3	35.0	104.5	102.3	46.51	46.51	0.812	0.824	0.97	0.81
5.0	60.0	36.4	119.0	35.0	121.6	118.4	43.19	43.66	0.992	0.993	0.95	0.80
10.0	40.0	16.1	60.9	20.0	61.0	60.6	64.88	66.43	0.654	0.629	0.98	0.83
10.0	40.0	19.4	66.3	40.0	66.7	66.1	64.06	65.36	0.650	0.630	0.98	0.83
10.0	40.0	25.2	69.8	20.0	69.6	68.1	62.27	63.60	0.663	0.630	0.98	0.83
10.0	40.0	28.5	74.8	40.0	74.9	73.9	60.98	62.67	0.665	0.630	0.98	0.83
10.0	40.0	36.3	82.3	35.0	83.2	79.5	62.04	60.62	0.657	0.631	0.98	0.83
10.0	50.0	16.9	75.5	20.0	78.0	76.8	62.07	61.76	0.811	0.826	0.97	0.82
10.0	50.0	23.8	80.8	40.0	82.9	85.5	60.95	59.87	0.812	0.826	0.97	0.82
10.0	50.0	25.1	83.1	20.0	85.3	83.5	59.85	59.53	0.812	0.826	0.97	0.82
10.0	50.0	29.0	88.8	40.0	90.8	89.8	58.39	58.56	0.813	0.827	0.97	0.82
10.0	50.0	36.5	94.8	35.0	97.1	95.2	56.35	56.83	0.810	0.827	0.97	0.82
10.0	60.0	17.9	91.1	20.0	94.6	93.6	58.13	57.47	1.000	1.017	0.96	0.81
10.0	60.0	25.4	91.5	40.0	99.6	102.9	57.12	55.68	1.001	1.019	0.96	0.81
10.0	60.0	31.4	104.3	40.0	107.4	107.9	54.82	54.38	1.006	1.019	0.96	0.81
10.0	60.0	36.4	110.4	35.0	113.8	111.1	53.14	53.37	1.008	1.020	0.96	0.81

A-5 Data set II-2

T_{evap} (°C)	T_{cond} (°C)	T_{suc} (°C)	T_{shell} (°C)	T_{amb} (°C)	$T_{dis,exp}$ (°C)	$T_{dis,cal}$ (°C)	$m_{r,exp}$ (kg/h)	$m_{r,cal}$ (kg/h)	W_{exp} (kW)	W_{cal} (kW)	h_v	h_c
-10.0	60.0	36.6	161.6	35.0	155.4	152.1	27.42	27.56	1.216	1.141	0.91	0.76
-5.0	40.0	5.5	75.7	20.0	79.4	79.2	47.49	45.69	0.868	0.852	0.96	0.83
-5.0	40.0	10.0	82.6	40.0	86.3	86.9	46.40	44.93	0.870	0.852	0.96	0.83
-5.0	40.0	13.7	83.0	20.0	86.9	85.7	45.83	44.33	0.871	0.852	0.96	0.83
-5.0	40.0	18.4	90.6	40.0	94.4	93.6	44.54	43.60	0.875	0.852	0.96	0.83
-5.0	50.0	6.7	95.3	20.0	95.3	98.2	42.93	41.68	1.043	1.030	0.94	0.81
-5.0	50.0	12.3	102.4	40.0	102.8	107.0	41.90	40.87	1.044	1.030	0.94	0.81
-5.0	50.0	14.1	103.3	20.0	103.2	103.9	41.39	40.62	1.042	1.030	0.94	0.81
-5.0	50.0	20.0	110.9	40.0	110.8	113.0	39.96	39.84	1.044	1.030	0.94	0.81
-5.0	60.0	6.3	114.0	20.0	116.8	117.1	37.49	38.20	1.183	1.208	0.92	0.78
-5.0	60.0	6.7	113.4	20.0	113.7	117.4	38.72	38.15	1.214	1.208	0.92	0.78
-5.0	60.0	11.9	123.0	40.0	126.6	126.1	35.57	37.51	1.194	1.208	0.92	0.78
-5.0	60.0	13.7	120.4	20.0	123.3	122.8	36.60	37.29	1.190	1.208	0.92	0.78
-5.0	60.0	19.4	130.8	40.0	134.1	131.9	34.56	36.64	1.202	1.208	0.92	0.78
0.0	50.0	36.5	114.9	35.0	115.4	116.0	49.06	47.28	1.065	1.065	0.95	0.82
2.5	50.0	15.0	86.9	20.0	91.1	91.4	58.20	56.81	1.049	1.077	0.96	0.83
2.5	50.0	17.0	90.2	30.0	94.6	94.8	56.95	56.38	1.053	1.077	0.96	0.83
2.5	50.0	18.9	93.4	40.0	97.2	98.0	56.33	55.98	1.054	1.077	0.96	0.83
5.0	50.0	16.9	87.0	40.0	87.8	91.6	64.86	62.91	1.096	1.085	0.96	0.83
5.0	50.0	17.1	84.7	20.0	89.3	88.8	63.21	62.86	1.055	1.085	0.96	0.83
5.0	50.0	19.2	89.2	30.0	90.0	92.1	64.52	62.34	1.095	1.085	0.96	0.83
5.0	50.0	21.8	91.9	40.0	93.0	95.8	63.14	61.73	1.099	1.085	0.96	0.83
5.0	50.0	23.3	91.8	30.0	94.0	95.6	63.39	61.38	1.093	1.086	0.96	0.83
5.0	50.0	25.0	94.5	40.0	98.8	98.6	60.82	61.00	1.063	1.086	0.96	0.83
5.0	50.0	36.6	104.4	35.0	109.1	107.5	57.92	58.56	1.064	1.086	0.96	0.83
5.0	60.0	36.5	124.8	35.0	126.8	125.6	53.85	54.16	1.311	1.314	0.95	0.81
10.0	40.0	16.8	62.6	20.0	65.8	63.2	83.02	84.85	0.858	0.827	0.98	0.85
10.0	40.0	19.7	67.4	40.0	69.9	68.0	81.50	83.71	0.857	0.827	0.98	0.85
10.0	40.0	25.5	70.6	20.0	74.3	70.7	79.06	81.59	0.860	0.828	0.98	0.85
10.0	40.0	28.5	75.7	40.0	78.9	75.8	77.48	80.56	0.861	0.828	0.98	0.85
10.0	50.0	16.7	76.6	20.0	77.8	79.8	77.97	78.08	1.091	1.087	0.97	0.84
10.0	50.0	20.3	80.9	40.0	82.1	85.4	76.99	76.87	1.093	1.088	0.97	0.84
10.0	50.0	25.6	86.4	20.0	87.6	87.5	75.04	75.20	1.090	1.088	0.97	0.84
10.0	50.0	29.6	91.2	40.0	92.5	93.5	73.41	74.02	1.093	1.089	0.97	0.84
10.0	50.0	36.5	95.9	35.0	100.6	98.8	70.98	72.12	1.067	1.089	0.97	0.84
10.0	60.0	16.8	94.0	20.0	98.1	97.4	71.75	71.89	1.288	1.344	0.96	0.83
10.0	60.0	20.1	98.6	40.0	103.4	102.9	69.74	70.93	1.295	1.345	0.96	0.83
10.0	60.0	25.5	102.2	20.0	106.5	105.0	68.53	69.45	1.294	1.346	0.96	0.83
10.0	60.0	28.8	107.1	40.0	112.1	110.6	66.87	68.60	1.302	1.346	0.96	0.83
10.0	60.0	36.4	114.7	35.0	117.2	116.4	67.04	66.77	1.342	1.347	0.96	0.83

A-6 Data set II-3

T_{evap} (°C)	T_{cond} (°C)	T_{suc} (°C)	T_{shell} (°C)	T_{amb} (°C)	$T_{dis,exp}$ (°C)	$T_{dis,cal}$ (°C)	$m_{r,exp}$ (kg/h)	$m_{r,cal}$ (kg/h)	W_{exp} (kW)	W_{cal} (kW)	h_v	h_c
-10.0	40.0	36.6	120.6	35.0	119.7	119.5	34.45	33.33	0.971	0.968	0.80	0.66
-10.0	60.0	37.1	185.4	35.0	173.8	177.6	23.78	24.67	1.499	1.470	0.66	0.49
-5.0	40.0	6.1	78.3	20.0	81.0	82.4	50.88	48.05	0.992	0.978	0.84	0.71
-5.0	40.0	10.9	85.2	40.0	87.7	90.8	49.63	47.16	0.992	0.979	0.84	0.71
-5.0	40.0	13.7	86.2	20.0	88.9	88.4	48.40	46.66	0.993	0.979	0.84	0.71
-5.0	40.0	18.8	93.3	40.0	95.4	97.0	47.29	45.79	0.991	0.979	0.84	0.71
-5.0	50.0	6.6	99.1	20.0	101.4	104.6	44.29	42.17	1.199	1.212	0.78	0.64
-5.0	50.0	12.1	107.5	40.0	109.3	114.0	41.39	41.33	1.200	1.213	0.78	0.64
-5.0	50.0	14.0	107.2	20.0	108.9	110.5	42.01	41.05	1.197	1.213	0.78	0.64
-5.0	50.0	19.9	114.9	40.0	116.6	120.1	41.43	40.21	1.196	1.213	0.78	0.64
-5.0	60.0	7.1	130.9	20.0	130.9	131.9	36.35	36.42	1.494	1.479	0.72	0.56
-5.0	60.0	13.5	140.4	40.0	141.3	142.5	34.76	35.63	1.492	1.480	0.72	0.56
-5.0	60.0	14.4	141.6	20.0	139.7	137.7	34.02	35.52	1.499	1.480	0.72	0.56
-5.0	60.0	20.9	149.1	40.0	149.1	148.4	33.57	34.78	1.505	1.480	0.72	0.56
0.0	50.0	36.3	119.3	35.0	121.4	119.9	48.80	49.08	1.213	1.231	0.82	0.69
2.5	50.0	15.3	91.1	20.0	94.4	94.4	61.11	59.78	1.220	1.234	0.84	0.71
2.5	50.0	17.6	94.0	30.0	97.1	98.1	60.51	59.24	1.219	1.234	0.84	0.71
2.5	50.0	19.5	97.2	40.0	100.4	101.6	60.18	58.81	1.224	1.234	0.84	0.71
5.0	40.0	36.6	90.7	35.0	93.8	90.9	67.44	68.94	0.975	0.963	0.90	0.78
5.0	50.0	17.1	89.1	40.0	92.4	94.0	69.08	66.92	1.227	1.235	0.85	0.73
5.0	50.0	19.3	91.0	30.0	94.4	94.2	66.94	66.33	1.222	1.236	0.85	0.73
5.0	50.0	21.5	93.5	40.0	96.8	97.8	66.54	65.75	1.221	1.236	0.85	0.73
5.0	50.0	23.3	95.0	30.0	98.5	97.7	64.99	65.29	1.221	1.236	0.85	0.73
5.0	50.0	25.7	98.1	40.0	101.4	101.4	64.42	64.69	1.220	1.237	0.85	0.73
5.0	50.0	36.4	108.3	35.0	111.7	109.5	61.48	62.20	1.223	1.238	0.86	0.73
5.0	60.0	36.5	133.7	35.0	136.7	131.1	53.22	55.55	1.554	1.527	0.81	0.67
10.0	40.0	16.9	62.4	20.0	65.3	63.3	93.29	93.79	0.949	0.924	0.92	0.81
10.0	40.0	20.6	66.7	40.0	69.1	69.0	92.02	92.14	0.950	0.925	0.92	0.81
10.0	40.0	25.3	70.7	20.0	74.0	70.6	87.45	90.17	0.948	0.925	0.92	0.81
10.0	40.0	29.2	75.2	40.0	78.1	76.6	86.43	88.64	0.947	0.926	0.92	0.81
10.0	50.0	16.6	78.1	20.0	81.4	80.5	86.47	84.69	1.222	1.226	0.88	0.76
10.0	50.0	20.7	82.9	40.0	86.2	86.7	84.25	83.14	1.219	1.227	0.88	0.76
10.0	50.0	25.4	86.7	20.0	90.6	88.2	79.73	81.48	1.210	1.228	0.88	0.76
10.0	50.0	29.3	91.6	40.0	95.1	94.3	78.91	80.18	1.210	1.228	0.88	0.76
10.0	50.0	36.3	98.5	35.0	102.3	99.7	75.22	78.00	1.209	1.229	0.88	0.76
10.0	60.0	17.0	99.2	20.0	102.7	100.2	76.17	75.77	1.554	1.536	0.84	0.71
10.0	60.0	20.9	103.0	40.0	107.3	106.5	75.63	74.53	1.549	1.537	0.84	0.71
10.0	60.0	25.3	107.0	20.0	117.7	107.5	71.99	73.22	1.545	1.539	0.84	0.71
10.0	60.0	29.2	113.4	40.0	116.9	113.9	70.13	72.11	1.554	1.540	0.84	0.71
10.0	60.0	36.3	120.2	35.0	123.8	119.4	67.96	70.24	1.555	1.541	0.84	0.71

A-7 Data set III-1

T_{evap} (°C)	T_{cond} (°C)	T_{suc} (°C)	T_{shell} (°C)	T_{amb} (°C)	$T_{dis,exp}$ (°C)	$T_{dis,cal}$ (°C)	$m_{r,exp}$ (kg/h)	$m_{r,cal}$ (kg/h)	W_{exp} (kW)	W_{cal} (kW)	h_v	h_c
-10.0	60.0	36.7	135.5	35.0	131.3	126.5	21.65	20.79	0.788	0.746	0.89	0.70
-5.0	40.0	6.6	69.0	20.0	71.5	69.4	32.60	33.04	0.593	0.569	0.95	0.76
-5.0	40.0	12.8	77.4	40.0	80.3	79.6	31.67	32.38	0.596	0.569	0.95	0.76
-5.0	40.0	14.0	74.7	20.0	77.4	74.3	32.27	32.25	0.592	0.569	0.95	0.76
-5.0	40.0	20.2	83.0	40.0	85.8	84.5	31.26	31.61	0.592	0.569	0.95	0.76
-5.0	50.0	7.1	81.3	20.0	83.6	84.3	30.78	30.79	0.687	0.686	0.93	0.74
-5.0	50.0	13.2	90.7	40.0	92.9	94.3	29.14	30.21	0.692	0.686	0.93	0.74
-5.0	50.0	14.0	92.5	20.0	89.2	88.7	30.92	30.14	0.692	0.686	0.93	0.74
-5.0	50.0	20.7	96.5	40.0	98.5	99.2	29.54	29.53	0.691	0.686	0.93	0.74
-5.0	50.0	31.1	105.1	40.0	106.5	105.8	31.65	28.64	0.693	0.687	0.93	0.74
-5.0	60.0	7.4	99.8	20.0	99.5	99.9	28.07	28.64	0.808	0.802	0.91	0.72
-5.0	60.0	7.7	98.3	20.0	99.4	100.1	27.16	28.61	0.799	0.802	0.91	0.72
-5.0	60.0	14.2	108.4	40.0	109.1	110.3	26.61	28.07	0.803	0.803	0.91	0.72
-5.0	60.0	14.4	105.2	20.0	104.7	104.2	27.95	28.05	0.804	0.803	0.91	0.72
-5.0	60.0	21.3	113.4	40.0	113.8	114.8	27.52	27.50	0.800	0.803	0.91	0.72
0.0	50.0	36.5	102.0	35.0	104.7	102.7	35.67	35.19	0.725	0.722	0.94	0.75
2.5	50.0	15.4	78.4	20.0	80.9	81.5	42.72	41.88	0.723	0.735	0.95	0.76
2.5	50.0	17.8	81.8	30.0	84.7	85.6	42.11	41.55	0.727	0.735	0.95	0.76
2.5	50.0	17.8	81.8	30.0	84.7	85.6	41.91	41.55	0.725	0.735	0.95	0.76
2.5	50.0	20.4	85.5	40.0	88.4	90.0	41.58	41.20	0.728	0.735	0.95	0.76
5.0	50.0	17.5	79.5	40.0	82.2	84.6	46.26	46.28	0.732	0.746	0.96	0.76
5.0	50.0	19.5	79.7	30.0	82.8	83.8	46.41	45.98	0.735	0.746	0.96	0.76
5.0	50.0	21.6	82.3	40.0	85.4	87.6	46.01	45.66	0.734	0.747	0.96	0.76
5.0	50.0	23.5	82.6	30.0	85.9	86.7	46.20	45.37	0.735	0.747	0.96	0.76
5.0	50.0	25.8	86.3	40.0	89.5	90.7	45.27	45.03	0.735	0.747	0.96	0.76
5.0	50.0	36.2	94.4	35.0	97.6	97.0	44.26	43.57	0.734	0.748	0.96	0.76
5.0	60.0	36.4	109.1	35.0	112.1	112.4	41.39	40.93	0.872	0.903	0.94	0.75
10.0	40.0	16.8	57.1	20.0	59.8	58.6	59.46	60.95	0.603	0.578	0.98	0.78
10.0	40.0	20.6	62.8	40.0	65.4	65.3	58.55	60.08	0.604	0.579	0.98	0.78
10.0	40.0	25.1	64.3	20.0	67.6	64.9	57.95	59.08	0.604	0.579	0.98	0.78
10.0	40.0	28.8	70.0	40.0	73.0	71.7	57.11	58.29	0.605	0.579	0.98	0.78
10.0	50.0	17.0	69.0	20.0	72.5	73.6	56.87	57.14	0.742	0.759	0.96	0.77
10.0	50.0	20.8	75.0	40.0	78.0	80.3	56.38	56.38	0.743	0.760	0.96	0.77
10.0	50.0	25.2	76.4	20.0	80.2	79.7	55.73	55.52	0.740	0.760	0.96	0.77
10.0	50.0	36.1	87.6	35.0	91.1	90.9	54.11	53.52	0.746	0.761	0.96	0.77
10.0	60.0	16.9	84.7	20.0	87.1	89.2	53.66	53.59	0.903	0.936	0.95	0.76
10.0	60.0	21.1	89.6	40.0	92.6	96.2	52.58	52.85	0.899	0.937	0.95	0.76
10.0	60.0	25.0	92.0	20.0	94.2	95.1	52.91	52.18	0.907	0.938	0.95	0.76
10.0	60.0	29.4	97.1	40.0	100.2	102.3	51.92	51.45	0.906	0.938	0.95	0.76
10.0	60.0	36.2	102.2	35.0	105.7	106.3	50.69	50.36	0.993	0.939	0.95	0.76

A-8 Data set III-2

T_{evap} (°C)	T_{cond} (°C)	T_{suc} (°C)	T_{shell} (°C)	T_{amb} (°C)	$T_{dis,exp}$ (°C)	$T_{dis,cal}$ (°C)	$m_{r,exp}$ (kg/h)	$m_{r,cal}$ (kg/h)	W_{exp} (kW)	W_{cal} (kW)	h_v	h_c
-10.0	45.0	36.6	106.0	35.0	108.0	102.4	27.96	26.78	0.683	0.658	0.94	0.70
-10.0	50.0	36.7	112.2	35.0	113.8	108.4	27.27	26.10	0.731	0.707	0.93	0.70
-10.0	54.4	36.7	118.6	35.0	119.3	113.8	26.32	25.50	0.770	0.749	0.92	0.70
-10.0	60.0	36.7	127.2	35.0	127.1	120.6	25.42	24.73	0.830	0.801	0.90	0.69
-5.0	40.0	5.7	67.3	20.0	69.4	67.6	37.05	37.98	0.667	0.639	0.96	0.71
-5.0	40.0	8.6	72.2	30.0	74.6	72.6	36.36	37.58	0.669	0.639	0.96	0.71
-5.0	40.0	11.2	76.4	40.0	78.3	77.5	35.80	37.23	0.668	0.639	0.96	0.71
-5.0	40.0	12.5	75.0	30.0	77.2	75.3	36.39	37.06	0.665	0.639	0.96	0.71
-5.0	40.0	16.5	79.4	30.0	81.6	77.9	35.55	36.54	0.665	0.640	0.96	0.71
-5.0	40.0	19.5	83.7	40.0	86.0	83.1	35.24	36.17	0.666	0.640	0.96	0.71
-5.0	50.0	8.8	84.8	30.0	86.3	85.9	35.10	35.69	0.779	0.760	0.94	0.70
-5.0	50.0	10.1	84.4	20.0	85.9	83.6	35.61	35.53	0.780	0.760	0.94	0.70
-5.0	60.0	9.2	100.2	30.0	101.3	99.5	32.12	33.77	0.893	0.873	0.92	0.70
-5.0	60.0	12.3	104.6	40.0	105.6	104.6	31.64	33.43	0.892	0.873	0.92	0.70
-5.0	60.0	17.2	107.3	30.0	108.6	104.6	31.86	32.91	0.891	0.874	0.92	0.70
-5.0	60.0	20.2	111.8	40.0	112.6	109.7	31.25	32.59	0.888	0.874	0.92	0.70
-1.5	45.0	11.4	73.4	25.0	76.1	76.0	41.82	42.21	0.737	0.725	0.96	0.71
-1.5	45.0	11.5	74.0	25.0	76.6	76.1	41.79	42.19	0.737	0.725	0.96	0.71
0.0	40.0	10.8	65.6	30.0	68.4	68.6	46.25	46.18	0.680	0.661	0.97	0.71
0.0	40.0	11.9	67.1	35.0	69.8	70.8	45.98	45.99	0.680	0.661	0.97	0.71
0.0	40.0	19.6	72.8	30.0	76.1	74.9	45.27	44.71	0.680	0.662	0.97	0.71
0.0	40.0	20.6	74.8	35.0	77.9	77.0	45.03	44.55	0.679	0.662	0.97	0.71
0.0	45.0	10.9	70.8	30.0	73.4	75.5	45.25	45.06	0.740	0.734	0.96	0.71
0.0	45.0	12.9	74.2	40.0	76.7	79.6	44.91	44.74	0.742	0.735	0.96	0.71
0.0	45.0	15.4	75.0	30.0	77.7	78.6	44.92	44.33	0.743	0.735	0.96	0.71
0.0	45.0	17.6	78.5	40.0	81.1	82.9	44.61	43.99	0.742	0.735	0.96	0.71
0.0	45.0	19.5	78.8	30.0	81.5	81.5	44.64	43.69	0.742	0.735	0.96	0.71
0.0	45.0	22.1	85.4	40.0	86.8	86.1	42.97	43.30	0.740	0.736	0.96	0.71
0.0	45.0	36.5	94.2	35.0	97.1	94.7	42.74	41.23	0.737	0.737	0.96	0.71
0.0	50.0	36.6	100.7	35.0	103.2	101.5	41.88	40.29	0.798	0.808	0.95	0.71
0.0	54.4	11.1	84.4	30.0	86.7	88.5	43.64	42.97	0.869	0.866	0.94	0.71
0.0	54.4	13.6	87.5	40.0	90.4	92.9	42.73	42.59	0.863	0.866	0.94	0.71
0.0	54.4	19.8	91.6	30.0	93.5	94.5	42.12	41.70	0.860	0.867	0.94	0.71
0.0	54.4	22.2	95.3	40.0	98.1	98.9	41.91	41.37	0.862	0.868	0.94	0.71
0.0	54.4	36.6	106.6	35.0	108.9	107.4	40.98	39.47	0.855	0.870	0.94	0.71
0.0	60.0	11.4	93.2	30.0	95.3	96.6	41.71	41.69	0.944	0.941	0.93	0.70
0.0	60.0	13.7	96.4	40.0	98.5	100.8	41.44	41.37	0.944	0.941	0.93	0.70
0.0	60.0	19.9	99.9	30.0	102.2	102.3	41.06	40.52	0.938	0.943	0.93	0.70
0.0	60.0	22.4	103.9	40.0	106.0	106.8	40.75	40.19	0.938	0.943	0.93	0.70
0.0	60.0	36.5	115.0	35.0	116.7	114.9	39.39	38.43	0.926	0.945	0.93	0.70

A-8 Data set III-2 (continue)

T_{evap} (°C)	T_{cond} (°C)	T_{suc} (°C)	T_{shell} (°C)	T_{amb} (°C)	$T_{dis,exp}$ (°C)	$T_{dis,cal}$ (°C)	$m_{r,exp}$ (kg/h)	$m_{r,cal}$ (kg/h)	W_{exp} (kW)	W_{cal} (kW)	h_v	h_c
2.0	40.0	11.9	62.8	30.0	65.6	67.1	49.21	50.00	0.683	0.667	0.97	0.71
2.0	40.0	14.6	64.2	20.0	67.4	66.5	49.08	49.49	0.684	0.667	0.97	0.71
2.0	50.0	10.4	73.6	20.0	76.4	77.2	47.78	47.91	0.820	0.820	0.95	0.71
2.0	50.0	16.9	81.3	30.0	84.0	84.4	46.87	46.80	0.820	0.821	0.95	0.71
2.0	50.0	23.2	87.3	40.0	90.0	91.5	46.55	45.78	0.813	0.822	0.96	0.71
2.0	60.0	19.3	97.6	40.0	100.3	102.6	44.36	44.17	0.958	0.967	0.94	0.70
2.0	60.0	21.1	98.1	30.0	101.0	101.3	44.59	43.91	0.959	0.968	0.94	0.70
5.0	45.0	14.4	67.7	30.0	71.0	72.2	54.11	54.73	0.758	0.756	0.97	0.71
5.0	45.0	16.3	71.3	40.0	74.2	76.0	53.35	54.34	0.758	0.756	0.97	0.71
5.0	45.0	18.8	71.5	30.0	74.8	75.5	53.94	53.83	0.756	0.756	0.97	0.71
5.0	45.0	20.8	74.9	40.0	78.1	79.3	53.40	53.43	0.759	0.757	0.97	0.71
5.0	45.0	23.0	76.0	30.0	79.1	78.6	53.32	53.00	0.755	0.757	0.97	0.71
5.0	45.0	25.1	79.1	40.0	82.3	82.5	52.61	52.60	0.754	0.757	0.97	0.71
5.0	50.0	14.8	74.9	30.0	78.3	79.5	52.37	53.36	0.833	0.840	0.96	0.71
5.0	50.0	15.4	76.0	35.0	79.1	81.1	52.63	53.24	0.833	0.840	0.96	0.71
5.0	50.0	16.3	77.5	40.0	80.7	83.0	52.31	53.07	0.834	0.840	0.96	0.71
5.0	50.0	19.8	80.1	35.0	83.2	84.4	52.09	52.39	0.827	0.841	0.96	0.71
5.0	50.0	19.8	80.0	35.0	83.2	84.4	51.82	52.39	0.826	0.841	0.96	0.71
5.0	50.0	19.9	80.7	35.0	83.7	84.4	51.83	52.37	0.832	0.841	0.96	0.71
5.0	50.0	20.0	80.5	35.0	83.4	84.5	51.62	52.36	0.829	0.841	0.96	0.71
6.0	55.0	22.7	87.3	35.0	90.5	92.4	53.46	52.74	0.910	0.931	0.96	0.71
6.0	55.0	22.9	87.0	35.0	90.4	92.6	53.48	52.70	0.908	0.931	0.96	0.71
10.0	40.0	17.8	56.9	30.0	60.2	61.6	67.76	67.59	0.686	0.661	0.98	0.72
10.0	40.0	18.0	58.1	30.0	61.4	61.7	66.02	67.54	0.698	0.661	0.98	0.72
10.0	40.0	18.4	58.1	35.0	60.9	63.1	67.49	67.43	0.687	0.661	0.98	0.72
10.0	40.0	19.5	60.8	40.0	63.9	64.9	65.57	67.13	0.698	0.661	0.98	0.72
10.0	40.0	26.9	65.7	30.0	69.2	68.7	66.06	65.19	0.685	0.662	0.98	0.72
10.0	40.0	27.6	66.6	35.0	70.0	70.2	66.18	65.01	0.686	0.662	0.98	0.72
10.0	40.0	28.7	69.4	40.0	73.0	72.1	63.81	64.74	0.696	0.662	0.98	0.72
10.0	40.0	29.8	66.3	30.0	69.8	70.9	64.19	64.46	0.683	0.662	0.98	0.72
10.0	45.0	18.1	63.7	30.0	67.1	68.9	65.20	65.98	0.764	0.761	0.97	0.72
10.0	45.0	19.7	66.6	40.0	69.8	72.1	64.52	65.56	0.764	0.762	0.97	0.72
10.0	45.0	22.6	67.9	30.0	71.6	72.3	64.06	64.83	0.761	0.762	0.97	0.72
10.0	45.0	24.2	70.7	40.0	74.1	75.6	63.97	64.43	0.764	0.762	0.97	0.72
10.0	45.0	27.0	72.2	30.0	76.1	75.7	63.17	63.74	0.762	0.763	0.97	0.72
10.0	45.0	28.6	74.8	40.0	78.4	79.0	62.72	63.36	0.761	0.763	0.97	0.72
10.0	45.0	36.3	80.4	35.0	84.4	83.9	63.17	61.58	0.760	0.764	0.97	0.72
10.0	50.0	18.2	70.0	30.0	73.7	76.1	63.62	64.43	0.846	0.860	0.97	0.71
10.0	50.0	19.0	71.5	35.0	75.2	77.7	63.25	64.24	0.848	0.860	0.97	0.71
10.0	50.0	19.6	72.8	40.0	76.0	79.2	63.26	64.09	0.849	0.860	0.97	0.71

A-8 Data set III-2 (continue)

T_{evap} (°C)	T_{cond} (°C)	T_{suc} (°C)	T_{shell} (°C)	T_{amb} (°C)	$T_{dis,exp}$ (°C)	$T_{dis,cal}$ (°C)	$m_{r,exp}$ (kg/h)	$m_{r,cal}$ (kg/h)	W_{exp} (kW)	W_{cal} (kW)	h_v	h_c
10.0	50.0	22.7	74.0	30.0	78.0	79.5	62.76	63.34	0.842	0.861	0.97	0.71
10.0	50.0	23.5	75.5	35.0	79.3	81.2	62.71	63.15	0.845	0.861	0.97	0.71
10.0	50.0	24.0	76.2	40.0	79.4	82.6	64.08	63.03	0.846	0.861	0.97	0.71
10.0	50.0	24.4	76.9	40.0	80.7	82.9	62.60	62.93	0.847	0.861	0.97	0.71
10.0	50.0	26.9	77.6	30.0	81.4	82.8	63.61	62.35	0.844	0.861	0.97	0.71
10.0	50.0	27.0	78.3	30.0	82.3	82.8	62.29	62.33	0.845	0.861	0.97	0.71
10.0	50.0	27.3	79.5	35.0	83.4	84.1	61.96	62.26	0.846	0.861	0.97	0.71
10.0	50.0	28.6	80.9	40.0	84.5	86.1	61.84	61.96	0.846	0.862	0.97	0.71
10.0	50.0	36.1	86.8	35.0	90.3	90.8	62.02	60.30	0.841	0.863	0.97	0.71
10.0	54.4	18.0	74.9	30.0	78.8	82.3	63.81	63.16	0.924	0.944	0.96	0.71
10.0	54.4	19.5	76.4	40.0	81.1	85.5	63.30	62.80	0.922	0.944	0.96	0.71
10.0	54.4	26.9	83.4	30.0	87.3	89.1	62.59	61.11	0.920	0.946	0.96	0.71
10.0	54.4	28.5	86.2	40.0	89.7	92.4	62.16	60.76	0.921	0.946	0.96	0.71
10.0	54.4	36.4	92.5	35.0	96.4	97.3	61.38	59.08	0.914	0.948	0.96	0.71
10.0	60.0	18.1	82.7	30.0	86.1	90.7	62.50	61.45	1.024	1.049	0.96	0.71
10.0	60.0	18.1	83.7	30.0	87.4	90.7	60.67	61.45	1.024	1.049	0.96	0.71
10.0	60.0	19.7	85.3	40.0	88.7	93.9	62.04	61.10	1.024	1.049	0.96	0.71
10.0	60.0	19.9	86.7	40.0	90.1	94.0	60.09	61.05	1.022	1.049	0.96	0.71
10.0	60.0	22.7	87.1	30.0	91.0	94.1	61.73	60.44	1.021	1.050	0.96	0.71
10.0	60.0	27.1	91.6	30.0	95.6	97.4	60.55	59.50	1.012	1.051	0.96	0.71
10.0	60.0	27.1	92.3	30.0	96.3	97.4	59.10	59.50	1.016	1.051	0.96	0.71
10.0	60.0	28.8	94.4	40.0	98.0	100.7	60.44	59.14	1.013	1.052	0.96	0.71
10.0	60.0	28.9	95.1	40.0	98.9	100.8	58.81	59.12	1.017	1.052	0.96	0.71
10.0	60.0	28.9	93.8	40.0	97.8	100.8	60.28	59.12	1.019	1.052	0.96	0.71
10.0	60.0	36.3	100.2	35.0	104.1	105.3	59.10	57.64	1.009	1.053	0.96	0.71

A-9 Data set III-3

T_{evap} (°C)	T_{cond} (°C)	T_{suc} (°C)	T_{shell} (°C)	T_{amb} (°C)	$T_{dis,exp}$ (°C)	$T_{dis,cal}$ (°C)	$m_{r,exp}$ (kg/h)	$m_{r,cal}$ (kg/h)	W_{exp} (kW)	W_{cal} (kW)	h_v	h_c
-10.0	60.0	36.3	137.8	35.0	138.4	141.1	40.85	39.72	1.371	1.347	0.87	0.60
-5.0	40.0	4.5	70.0	20.0	71.7	74.3	60.63	61.33	1.047	1.014	0.94	0.67
-5.0	40.0	11.3	78.3	40.0	81.6	80.3	59.43	59.73	1.044	1.015	0.94	0.67
-5.0	40.0	12.9	76.1	20.0	78.3	81.6	59.08	59.37	1.046	1.015	0.94	0.67
-5.0	40.0	19.1	85.9	40.0	87.8	88.1	57.98	58.01	1.045	1.016	0.94	0.67
-5.0	50.0	5.8	83.1	20.0	88.2	87.8	58.34	58.29	1.230	1.223	0.92	0.65
-5.0	50.0	11.2	90.0	40.0	97.0	94.4	56.77	57.13	1.227	1.224	0.92	0.65
-5.0	50.0	13.6	90.1	20.0	94.3	95.2	56.87	56.63	1.226	1.225	0.92	0.65
-5.0	50.0	18.8	96.7	40.0	103.0	101.5	55.94	55.58	1.228	1.227	0.92	0.65
-5.0	60.0	4.1	100.2	20.0	103.3	105.5	54.95	55.71	1.472	1.430	0.89	0.62
-5.0	60.0	6.1	101.0	20.0	104.8	104.9	54.30	55.30	1.443	1.431	0.89	0.62
-5.0	60.0	12.1	110.3	40.0	114.1	111.9	53.17	54.13	1.448	1.434	0.89	0.62
-5.0	60.0	13.0	108.2	20.0	110.2	113.5	53.43	53.96	1.479	1.434	0.89	0.62
-5.0	60.0	20.2	117.4	40.0	120.4	119.2	53.53	52.62	1.447	1.437	0.89	0.62
0.0	50.0	36.2	104.5	35.0	108.7	109.4	65.64	64.63	1.271	1.289	0.93	0.66
2.5	50.0	14.9	81.0	20.0	85.0	85.1	76.96	77.46	1.287	1.306	0.94	0.67
2.5	50.0	15.8	83.6	30.0	87.5	87.5	77.11	77.19	1.298	1.306	0.94	0.67
2.5	50.0	17.3	83.6	30.0	88.8	87.6	76.29	76.75	1.286	1.307	0.94	0.67
2.5	50.0	17.4	85.4	30.0	88.9	87.5	76.67	76.72	1.290	1.307	0.94	0.67
2.5	50.0	19.7	85.8	40.0	92.6	89.9	76.47	76.05	1.286	1.308	0.94	0.67
5.0	50.0	17.2	80.1	40.0	86.7	83.8	85.10	85.02	1.304	1.325	0.94	0.68
5.0	50.0	19.1	81.2	30.0	86.7	85.5	84.23	84.38	1.302	1.326	0.94	0.68
5.0	50.0	21.4	83.6	40.0	90.3	87.6	84.07	83.63	1.302	1.327	0.94	0.68
5.0	50.0	23.1	84.9	30.0	90.0	89.3	83.69	83.09	1.305	1.328	0.94	0.68
5.0	50.0	25.3	87.3	40.0	93.5	91.4	83.38	82.39	1.309	1.328	0.94	0.68
5.0	50.0	36.1	97.4	35.0	101.7	102.2	79.86	79.17	1.310	1.332	0.94	0.68
5.0	60.0	28.5	102.8	40.0	112.1	111.8	80.06	78.13	1.583	1.604	0.92	0.66
5.0	60.0	36.1	112.6	35.0	117.5	117.6	76.64	76.05	1.570	1.608	0.92	0.66
10.0	40.0	16.5	59.2	20.0	60.6	62.3	106.80	108.00	1.077	1.027	0.97	0.70
10.0	40.0	20.7	64.5	40.0	67.0	69.7	105.70	106.10	1.073	1.028	0.97	0.70
10.0	40.0	25.3	66.0	20.0	68.1	70.6	103.60	104.10	1.080	1.029	0.97	0.70
10.0	40.0	30.3	73.2	40.0	75.3	75.2	101.30	102.00	1.081	1.031	0.97	0.70
10.0	50.0	16.6	71.2	20.0	75.9	75.0	103.60	104.00	1.322	1.346	0.95	0.69
10.0	50.0	20.5	75.9	40.0	82.0	79.1	102.30	102.40	1.326	1.347	0.95	0.69
10.0	50.0	24.8	78.8	20.0	82.8	83.2	100.80	100.60	1.326	1.349	0.96	0.69
10.0	50.0	28.9	83.7	40.0	89.2	87.8	99.16	98.98	1.327	1.351	0.96	0.69
10.0	50.0	36.0	90.3	35.0	94.6	94.7	96.63	96.30	1.331	1.353	0.96	0.69
10.0	60.0	16.9	88.4	20.0	92.0	90.7	99.44	99.79	1.620	1.656	0.94	0.67
10.0	60.0	21.8	92.9	40.0	98.9	95.1	97.41	97.87	1.620	1.660	0.94	0.67
10.0	60.0	25.0	94.8	20.0	98.8	99.0	96.59	96.65	1.649	1.662	0.94	0.67
10.0	60.0	36.0	105.2	35.0	110.2	109.8	93.02	92.74	1.625	1.668	0.94	0.67